Laser-Driven Dielectric-Structure Accelerators*

Eric R. Colby†

Accelerator Research Department B
SLAC

* http://www-project.slac.stanford.edu/e163/DielectricAccelTalk.pdf

† ecolby@slac.stanford.edu

Work supported by Department of Energy contracts DE-AC03-76SF00515 (SLAC) and DE-FG03-97ER41043-II (LEAP).

The LEAP & E163 Collaborators

C. D. Barnes, E. R. Colby, B. M. Cowan, M. Javanmard, R. J. Noble,
D. T. Palmer, C. M. Sears, R. H. Siemann, J. E. Spencer, D. R. Walz
Stanford Linear Accelerator Center

R. L. Byer, T. Plettner, J. A. Wisdom
Stanford University

T. I. Smith, R. L. Swent
Hansen Experimental Physics Laboratory

Y.-C. Huang
National Tsing Hua University, Taiwan

L. Schächter
The Technion
Israeli Institute of Technology, Haifa

Why is laser-driven acceleration in "vacuum" worth pursuing?

"Vacuum":

- No plasmas, background gases; only solid objects
- Low-field $a_o = eE/2\omega mc \ll 1$

Physical and Technical Issues

What are the most promising laser acceleration methods?

Crossed-Gaussian Accelerator

Photonic Band Gap Accelerator

→Laser-Driven Linear Collider Concept

What R&D is needed to make a working laser accelerator?

STELLA

Laser Electron Accelerator Project (LEAP)

E163, SPRC, and follow-on programs at ORION

General Roadmap

Three Questions

Requirements for Future High Energy Linear Colliders

Near Term:

- Center-of-mass energy 0.5-1.0 TeV
- Luminosity >10^{34} cm^{-2} s^{-1}

Long Term:

- >3 TeV and readily extendable
- Luminosity >10^{35} cm^{-2} s^{-1} and increasing with γ^2

Compactness, power efficiency, reliability, affordability

Linear optical-wavelength acceleration requires:

Sub-femtosecond electron bunches → sub-fs radiation pulses

Very small emittance beams → radiation sources are truly point-like

High Power Density → High Field Strength

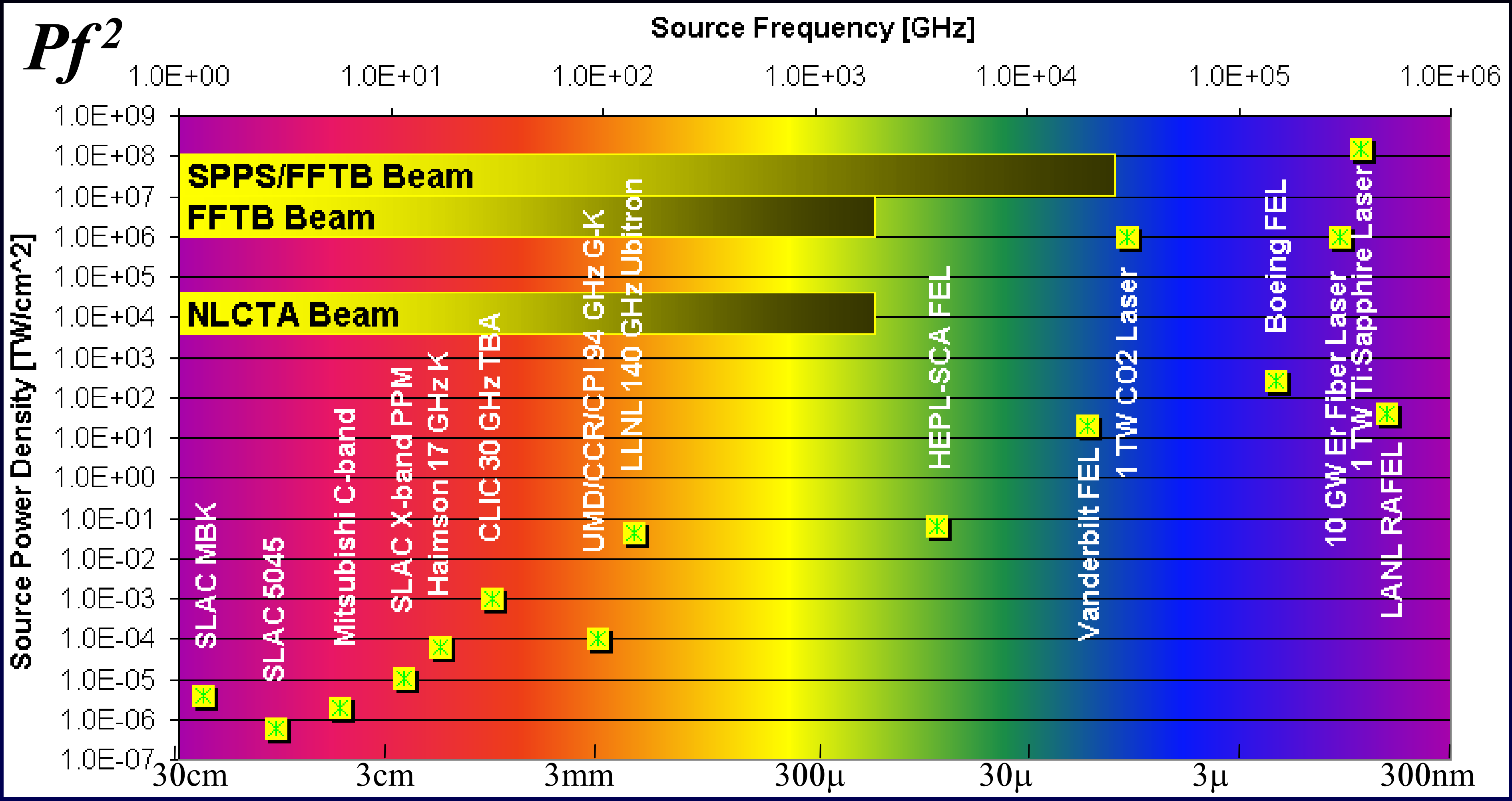

Source Wavelength

*28.5 GeV, 1e10 ppp, 1μ x 1μ x 600μ (20μ for SPPS) beam

**350 MeV, 1e10 ppp, 1μ x 1μ x 1 mm beam

Short-Pulse Optical Damage of Dielectrics

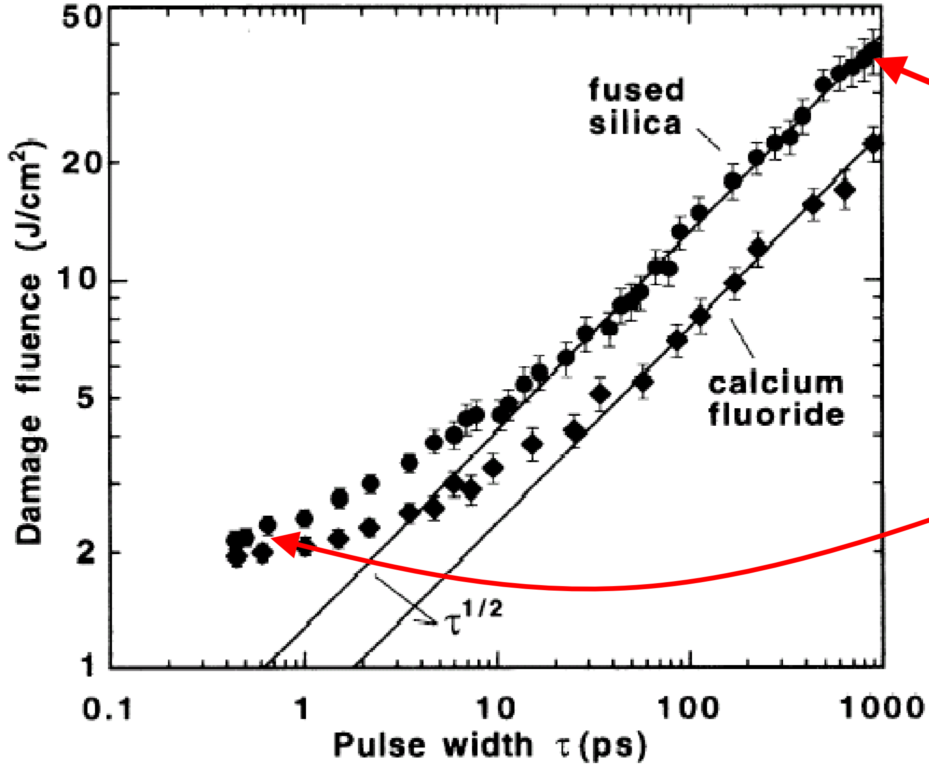

FIG. 1. Observed values of damage threshold at 1053 nm for fused silica (●) and CaF_2 (◆). Solid lines are $\tau^{1/2}$ fits to long pulse results. Estimated uncertainty in the absolute fluence is ±15%.

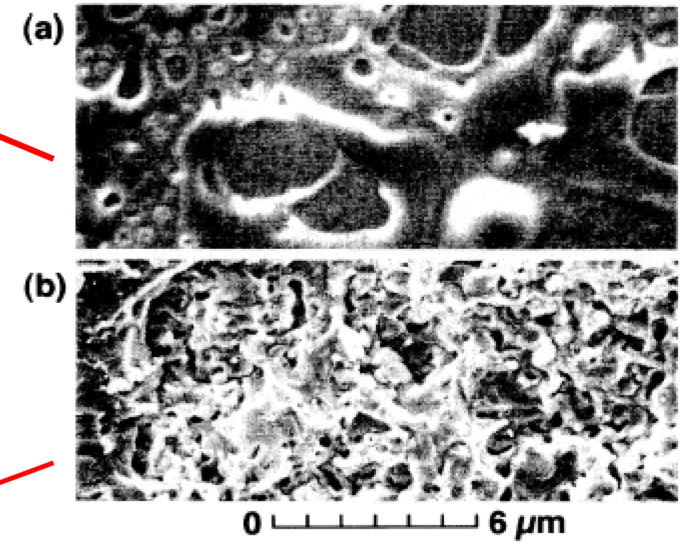

FIG. 2. Scanning electron micrograph of front-surface damage of fused silica produced by 1053 nm pulses of duration (a) 900 ps, showing melting, and (b) 500 fs, showing ablation and fracture.

B. C. Stuart, *et al*, "Laser-Induced Damage in Dielectrics with Nanosecond to Subpicosecond Pulses," *Phys. Rev. Lett.*, **74**, p.2248ff (1995).

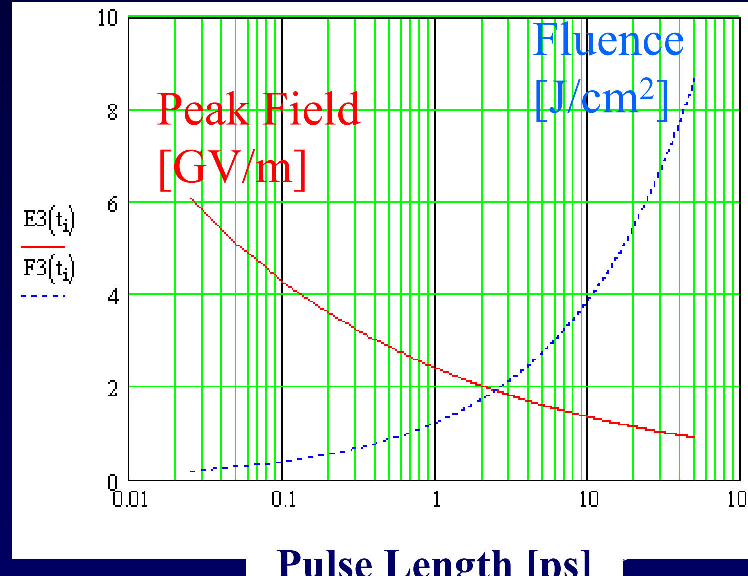

Electrical Efficiency of Coherent Power Sources

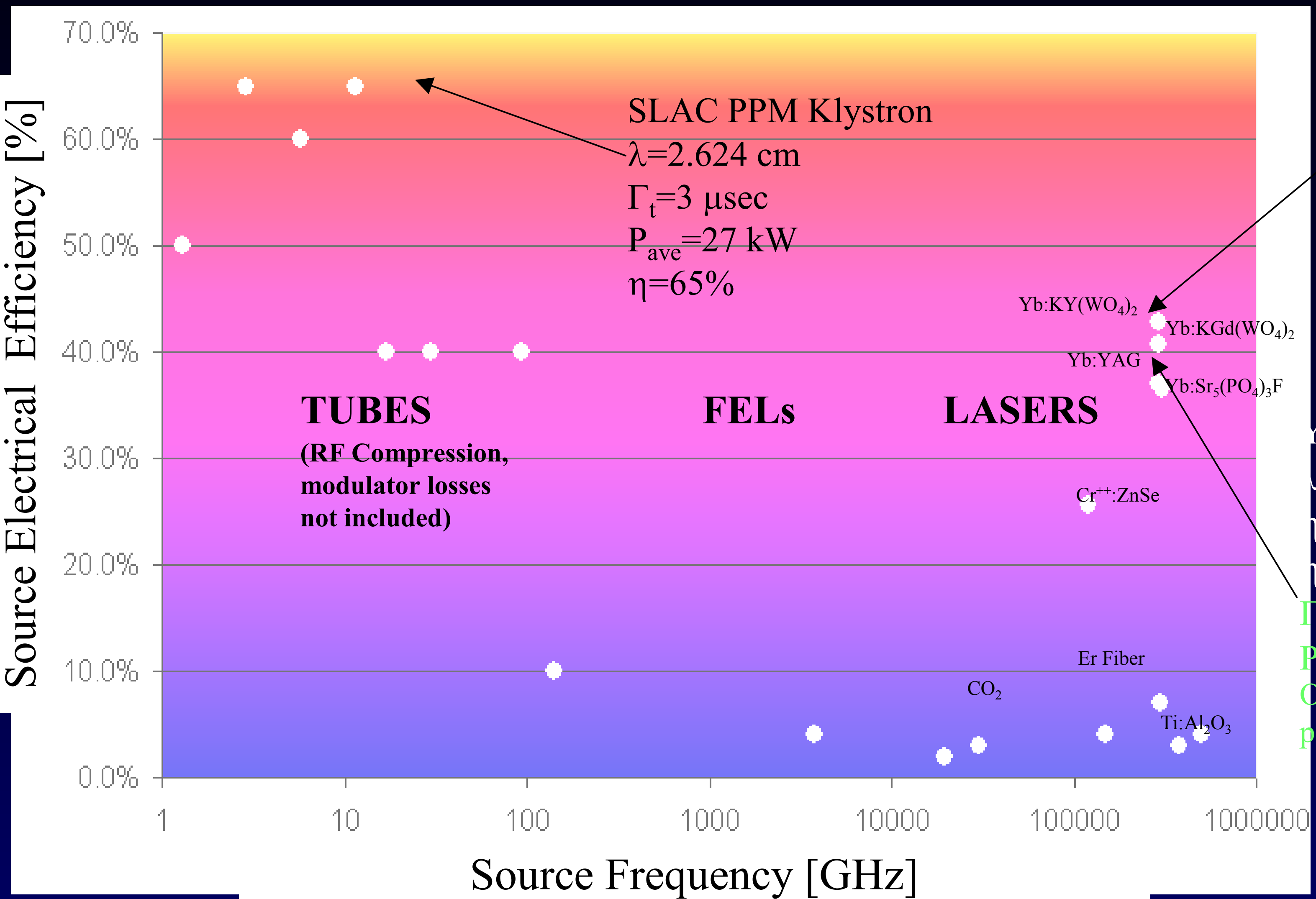

Yb:KY(WO$_4$)$_2$
λ=1.028μ
η_{slope}=86.9%
η_a=22%
η_ε=43% (theoretical)
Γ_t=240 fsec
P_{ave}=22.0 W
Opt. Lett., **27** (13), p.1162, July (2002).

Yb:KGd(WO$_4$)$_2$
λ=1.023μ
η_{slope}=82.7%
η_ε=41% (theoretical)
Γ_t=176 fsec
P_{ave}=1.1 W
Opt. Lett., **25** (15), p.1119, August (2000).

Commercially Available High Efficiency Laser Diode Bars

nLIGHT PHOTONICS

Preliminary Data Sheet | **NL-SAG**

300W (cw), η_e=50%, λ=780-1000 nm

High Power Stacks

nLight Photonics' high power stacked bar module provides state-of-the-art power levels in a compact package. Starting with high power diode 1 cm bars, multiple modules are stacked to provide extremely high output power. These modules are water cooled to maximize output power without sacrificing the lifetime of the diode.

Optical	
Center Wavelength (Range)	780-1000nm
CW Output Power	300W (6 plates)
Center Wavelength Tolerance	±3.0nm
Array Length	1cm
Electrical	
Total Conversion Efficiency	50%
Threshold Current	10A
Operationg Current	60A
Operating Voltage	< 12V
Series Resistance	0.04Ω
Thermal	
Thermal Resistance	0.35°C/W
Operating Temperature	10°C to 40°C
Fluid Flow Rate	300 ml/min/plate
Inlet to Outlet presure drop	30 psi
Deionized Water Resistivity	.5 – 2Mohm-cm
Filter	< 20μm

CEO CUTTING EDGE OPTRONICS

3900 W, η_e=40%, λ=792-812 nm, (585 W ave.)

Z PACKAGE

- Packaged 112 Bar Laser Diode Array
- Other Powers Are Also Available
- Available Wavelengths 785-1064nm

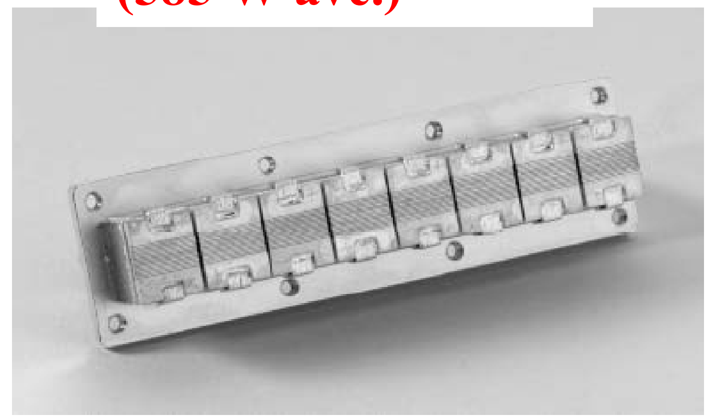

OPTICAL CHARACTERISTICS

PARAMETER	CONDITIONS	MIN	TYP	MAX	UNITS
QCW Peak Power Output	60A, 150 μsec, 1 kHz	3900	---	---	W
Operating Current	3900W at 25°C Heat Sink	---	55	60	A
Threshold Current	25°C Heat Sink	---	13	16	A
Slope Efficiency	25°C Heat Sink	106.4	123.2	---	W/A
Efficiency	3900W at 25°C Heat Sink	35	40	---	%
Number of Emitters	---	---	72 x 112	---	
Emitter Size	---	---	90 x 1	---	μm
Emitter Pitch	---	---	133.3	---	μm
Center Wavelength	3900W at 25°C Heat Sink	792	808	812	nm
Wavelength Tolerance	3900W at 25°C Heat Sink	± 1	± 3	± 4	nm
Spectral Width	3900W at 25°C Heat Sink	---	4.0	5.0	nm
Wavelength Shift	---	0.23	0.25	0.27	nm/°C
Beam Divergence FWHM (1)	---	---	40x10	42x12	° x °
Polarization	---	---	TE	---	---
Degradation Rate (2)	25°C Heat Sink	---	5	---	%/G shots

ELECTRICAL CHARACTERISTICS

PARAMETER	CONDITIONS	MIN	TYP	MAX	UNITS
Built-In Voltage	25°C Heat Sink	---	179.2	190.4	V
Series Resistance	25°C Heat Sink	---	0.896	1.344	ohms
Operating Voltage	25°C Heat Sink, 3900W	---	224	257.6	V

U.S. Patent Numbers: 5,734,672 5,913,108

NOTES

(1) Lower beam divergence is also available.

(2) Typical degradation rates are 5% in the first 10 million shots and 5% per billion shots thereafter.

Cutting Edge Optronics • 20 Point West Blvd. • St. Charles, MO 63301

636.916.4900 • 636.916.5665 fax • www.ceolaser.com

Stable optical phase-locking to a microwave reference has been demonstrated.

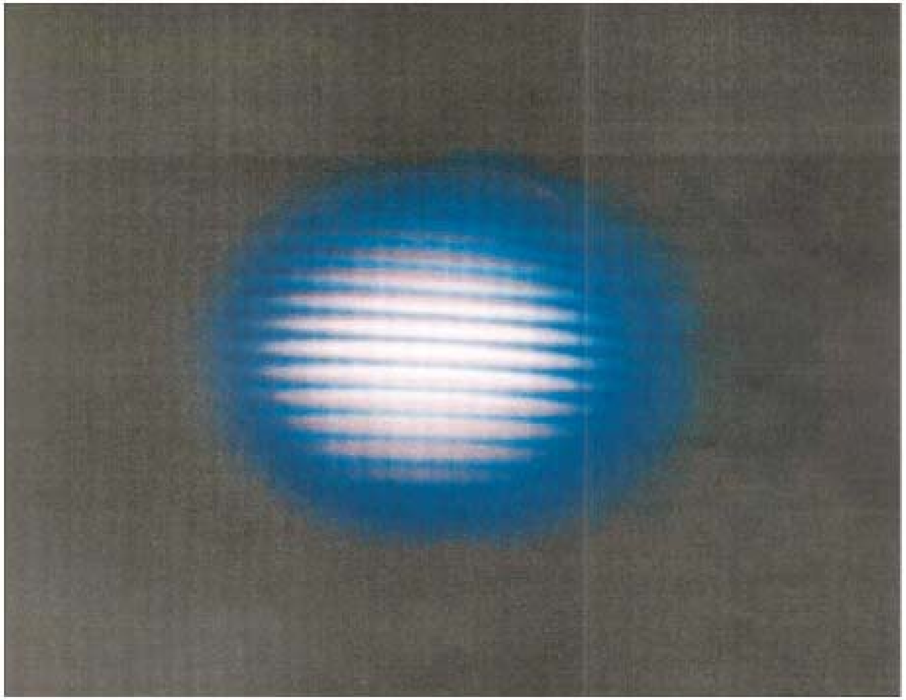

Fig. 2. White-light fringes resulting from the interference of the two continua generated by the two phase-locked IR laser pulses when the relative delay is properly adjusted to zero.

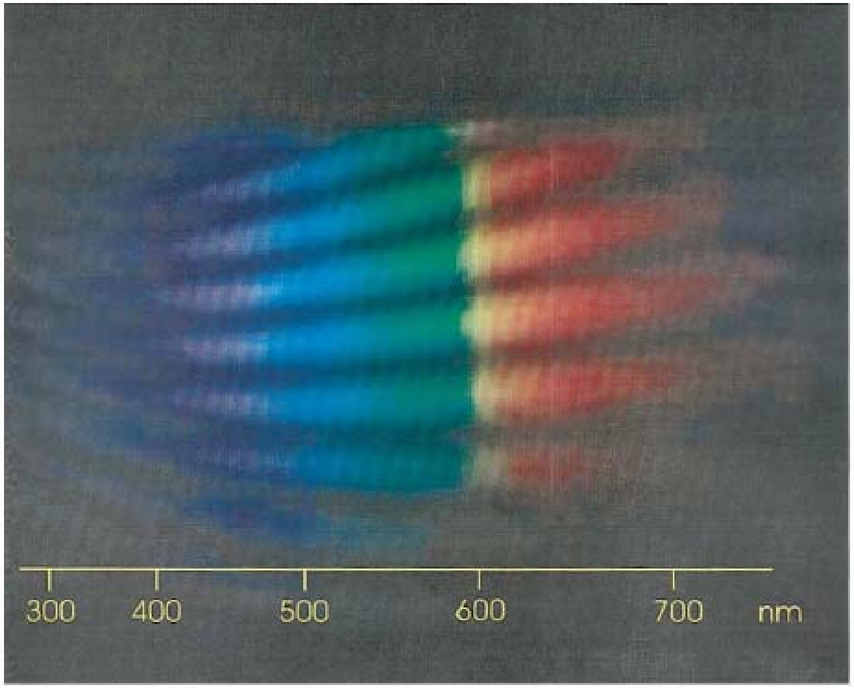

Fig. 3. Spectrally dispersed white-light fringes. Clear and well-defined fringes indicate that a stable phase relationship is conserved across all the generated visible spectrum.

Interference fringes of carrier phase-locked white light continua generated from a Ti:Sapphire laser.

M. Bellini, T Hansch, Optics Letters, **25** (14), p.1049, (2000).

Laser development is strongly driven by industry

- Lasers are a $4.8B/year market (worldwide), with laser diodes accounting for 59%, DPSS lasers $0.22B/year, and CO_2 lasers $0.57B/year [1] (in contrast, the domestic microwave power tube market is $0.35B/year, of which power klystrons are just $0.06B/year[2]).

- Peak Powers of TW, average powers of kW are available from commercial products

- The market's needs and accelerator needs overlap substantially: Cost, reliability, shot-to-shot energy jitter, coherence, mode quality are needed by both

[1] K. Kincade, "Review and Forecast of the Laser Markets", Laser Focus World, p. 73, January, (2003).

[2] "Report of Department of Defense Advisory Group on Electron Devices: Special Technology Area Review on Vacuum Electronics Technology for RF Applications", p. 68, December, (2000).

Fundamental Physics Considerations I

- Lawson-Woodward Theorem requires that one or more of:
  - Boundaries*
  - Gases
  - Periodic transverse motion of accelerated particles

  be present for linear acceleration ($\propto E$) to take place

- *Furthermore, since free-space modes are strictly TEM, efficient acceleration requires a structure that either strongly diffracts the TEM mode, or guides a TM-like mode ➔ boundaries must be very close to the beam ($r/\gamma\lambda<1$)

- Accelerating fields must not degrade transverse emittances → fields must be rotationally symmetric

Fundamental Physics Considerations II

- Good coupling impedance → strong fundamental-mode wakefield
- Stability against regenerative beam breakup → minimal higher order mode wakefields
- Higher stored energy (Q) in structure → Tighter dimensional tolerances

- Larger acceptance → larger aperture

Basic Technical Considerations I

- For efficiency, accelerators should be designed at wavelengths to use the most efficient lasers
  - Yb:KGd$(WO_4)_2$, Yb:KY$(WO_4)_2$ → $\lambda \sim 1.0\ \mu m$
  - Erbium Fiber → $\lambda \sim 1.5\ \mu m$
  - Cr^{++}:ZnSe → $\lambda \sim 2.2$-$2.8\ \mu m$

- For economy of fabrication, accelerators should be designed at wavelengths were materials are low loss and amenable to lithographic or fiber drawing processes:
  - a-SiO_2 → $\lambda \sim 0.2$-$2.5\ \mu m$
  - c-Si → $\lambda > 1.5\ \mu m$

Basic Technical Considerations II

- Structure materials should have
  - High damage threshold → resistance to breakdown
  - High radiation resistance → resistance to high-radiation accelerator environment
  - Excellent optical linearity, even under large applied electric fields → minimal intensity-dependent dephasing
  - Good thermal conductivity, low thermal expansion → thermally stable under changing operating conditions
  - Amenability to fabrication → Lithography or fiber drawing

Short-Pulse Laser Damage of Dielectrics

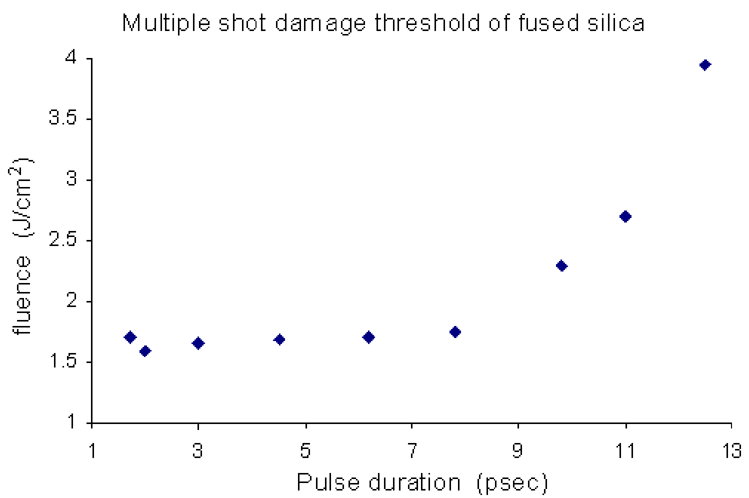

- $t^{1/2}$ dependence for t>10 ps
- No t dependence for t<5 ps
- "Laser Conditioning" raises threshold ~10%
- Some materials perform worse under vacuum

Fields for σ_t=1 ps

1.7 GV/m

1.2 GV/m

material	damage threshold	
	air	vacuum
CaF_2	2.212	2.260
borofloat	2.064	2.054
fused silica	2.027	1.795
sapphire	1.574	1.152
MgF_2	1.455	1.455
800 nm HR	0.769	0.768
$LiNbO_3$	0.504	0.194

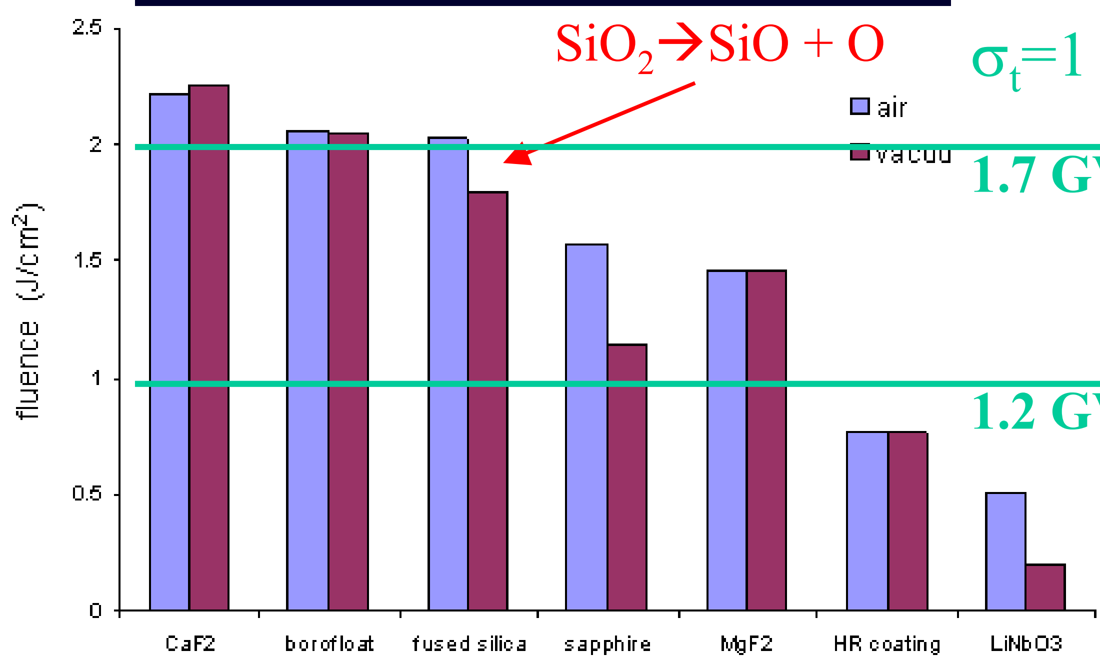

T. Plettner, "Proof-of-Principle Experiment for Crossed Laser beam Electron Acceleration in a Dielectric Loaded Vacuum Structure", Ph.D. Thesis, Stanford Univ., 2002.

Radiation Resistance of Dielectrics

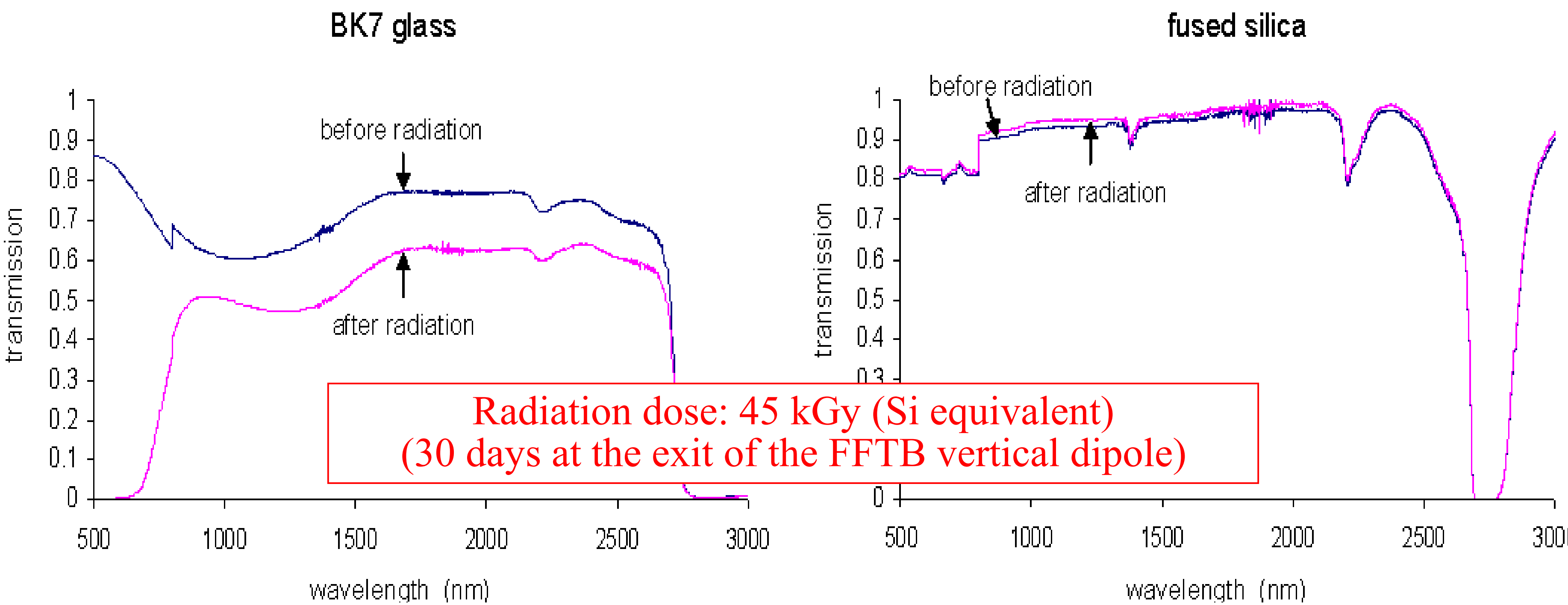

J. Spencer, *et al*, “Gamma Radiation Studies on Optical Materials”, to be published in *IEEE Trans. Nucl. Science*, (2002).

Gamma-resistant Materials (no measurable change in transmission characteristics in the 0.8-3 μm range for a dose exceeding 100 kGy Si equivalent from a Co^{60} source): $c\text{-}SiO_2$, c-Si , c-GaAs , Nd:YAG

Neutron damage studies (with a Cf^{252} source) are planned.

Progress in Precision Lithography

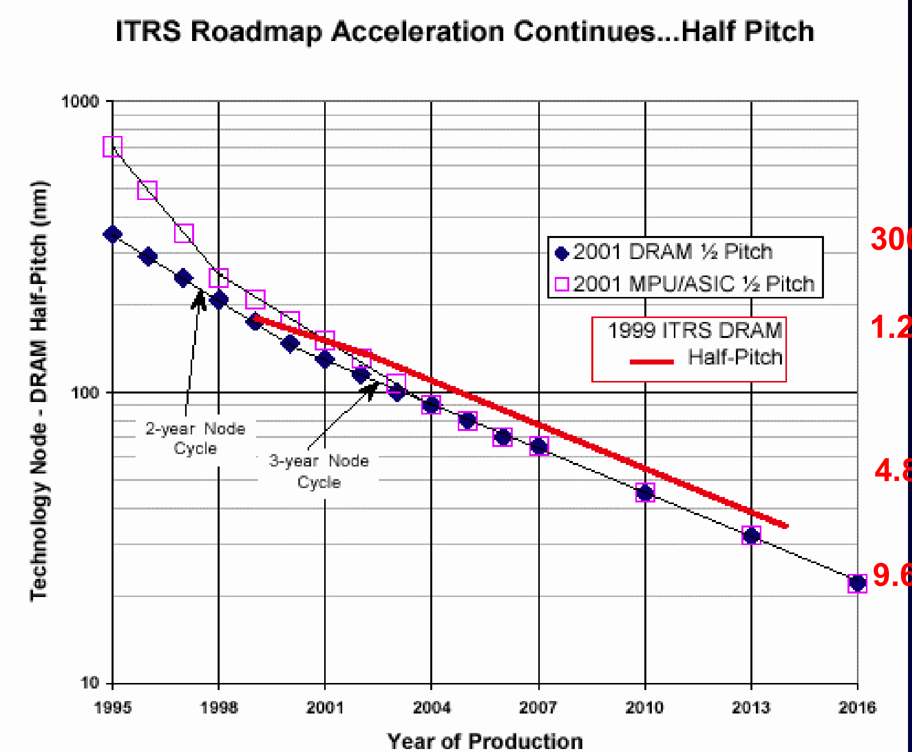

Source: 2001 ITRS - Exec. Summary, ORTC Figure

Dense, λ/10-sized features possible by standard semiconductor lithography

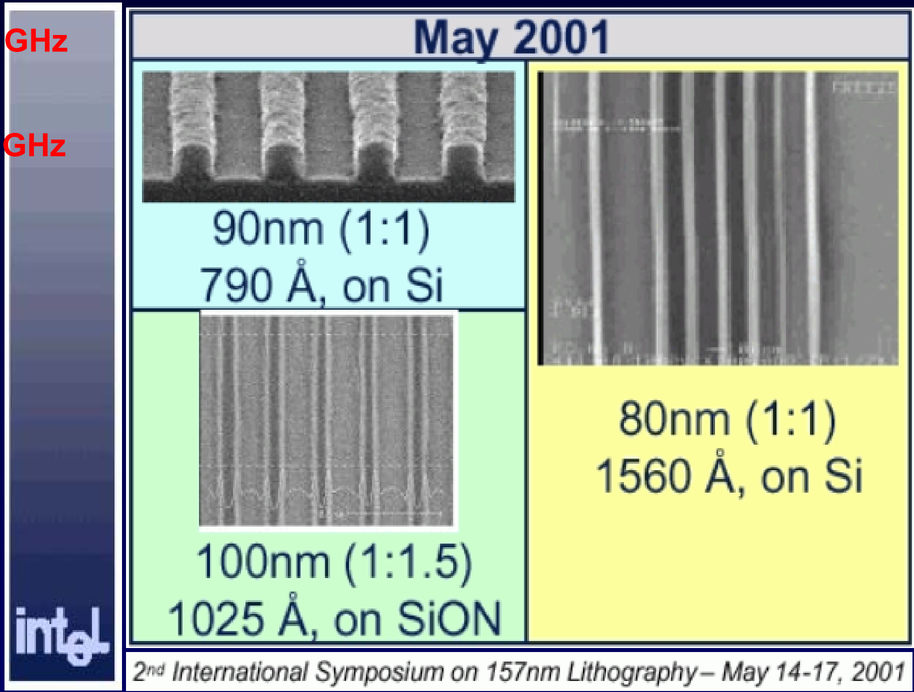

Fiber Bundle Drawing

http://www.crystal-fibre.com

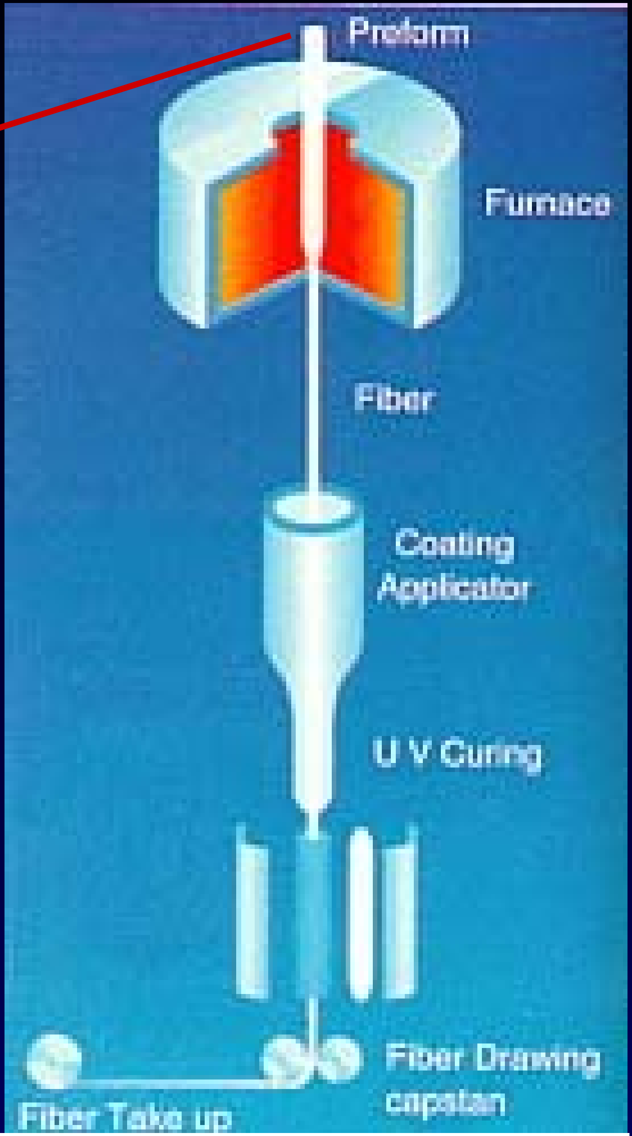

http://www.infodotinc.com/neets/tm/107-5.htm

http://www.tegs.ru/images/big/028.jpg

- Preform has essentially the same geometry as the finished bundle
- Dimensional drawdowns of 1000:1 routine

Examples of Dielectric Laser Accelerator Structures

First Example: Interferometric Acceleration (Inverse Transition Radiation Acceleration)

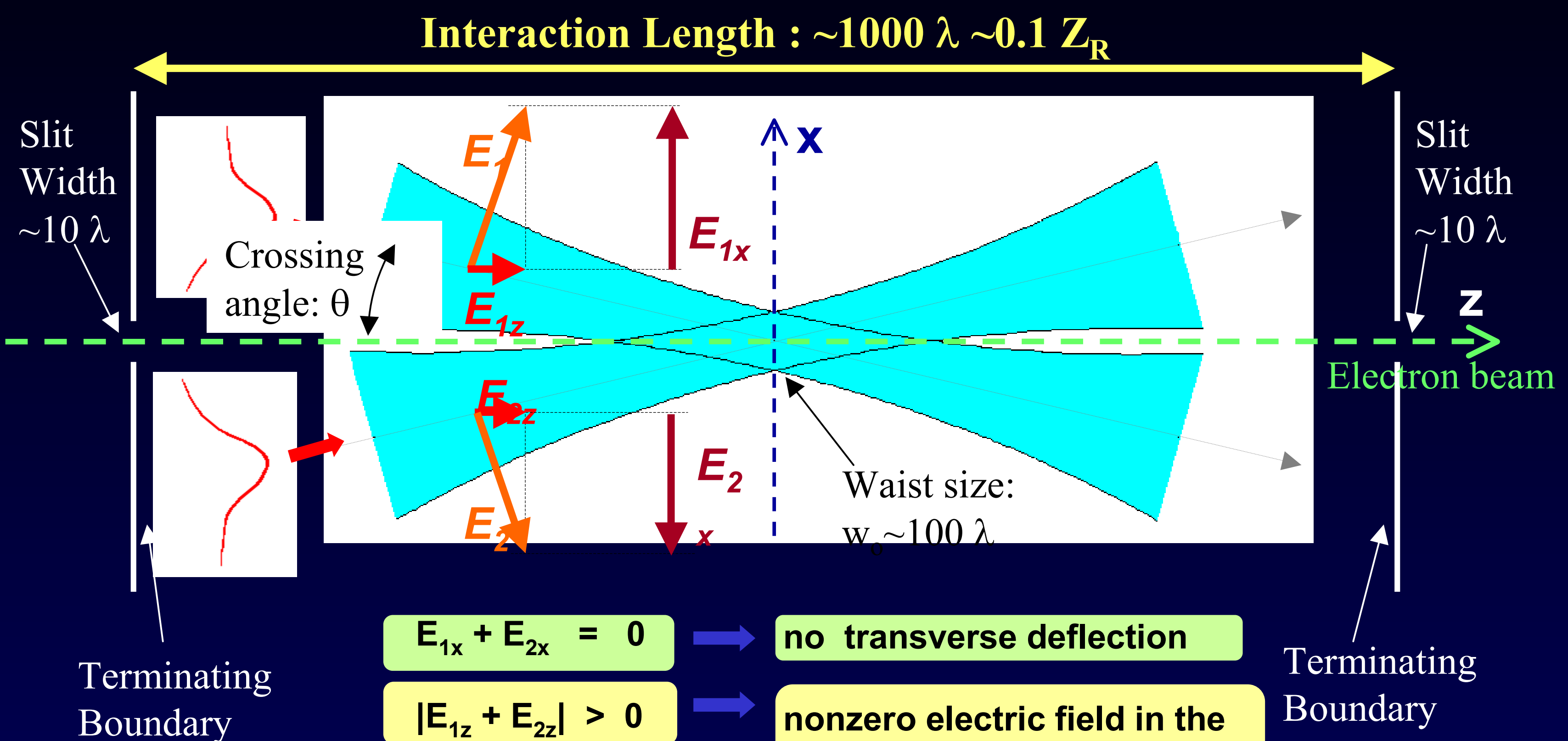

$E_{1x} + E_{2x} = 0$ → no transverse deflection

$|E_{1z} + E_{2z}| > 0$ → nonzero electric field in the direction of propagation

The laser beams are polarized in the XZ plane, and are out of phase by π

Gradient limited to ≲70 MeV/m for γ→ ∞ [R. Noble, 2001].

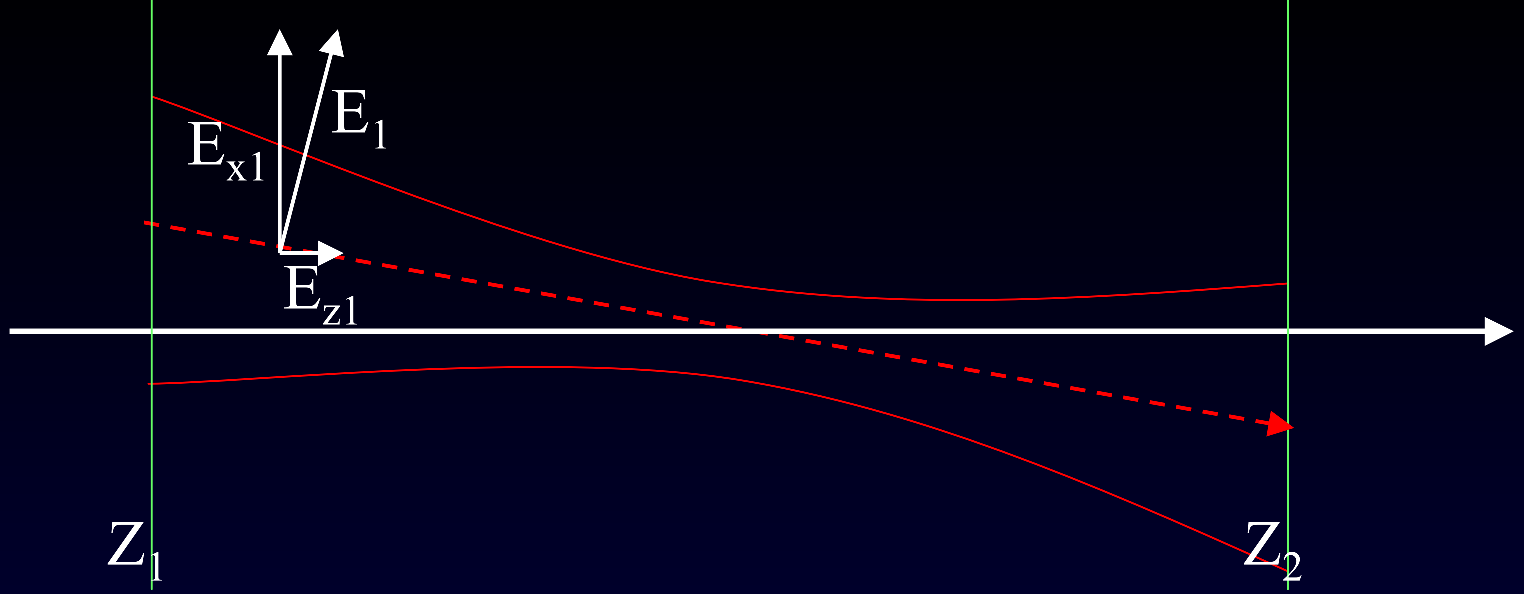

$$E_{x1} = \frac{E_{01} w_o}{w_1} \exp\left[-\frac{r_1^{\,2}}{w_1^2}\right] \cos(\psi_t)$$

$$E_{z1} = \frac{2E_{01} x_1}{k w_1^{\,2}} \exp\left[-\frac{r_1^{\,2}}{w_1^2}\right] \left(\sin(\psi_t) - \left[\frac{z_1}{Z_R}\right] \cos(\psi_t)\right)$$

(paraxial approximation to first order in $1/w_o k \sim 10^{-3}$)

$$\psi_t = kz_1 - \omega t + z_1 r_1^{\,2} / (Z_R w_1^{\,2}) - \tan^{-1}(z_1 / Z_R) + \phi_o$$

P. Sprangle, E. Esarey, J. Krall, A. Ting, *Opt. Comm.*, **124**, p.69ff, (1996).

The LEAP Cell

(Numerical Integration)

E_z[MV/m]

E_x[kV/m]

E_z[MV/m]

(SEK, analytic)

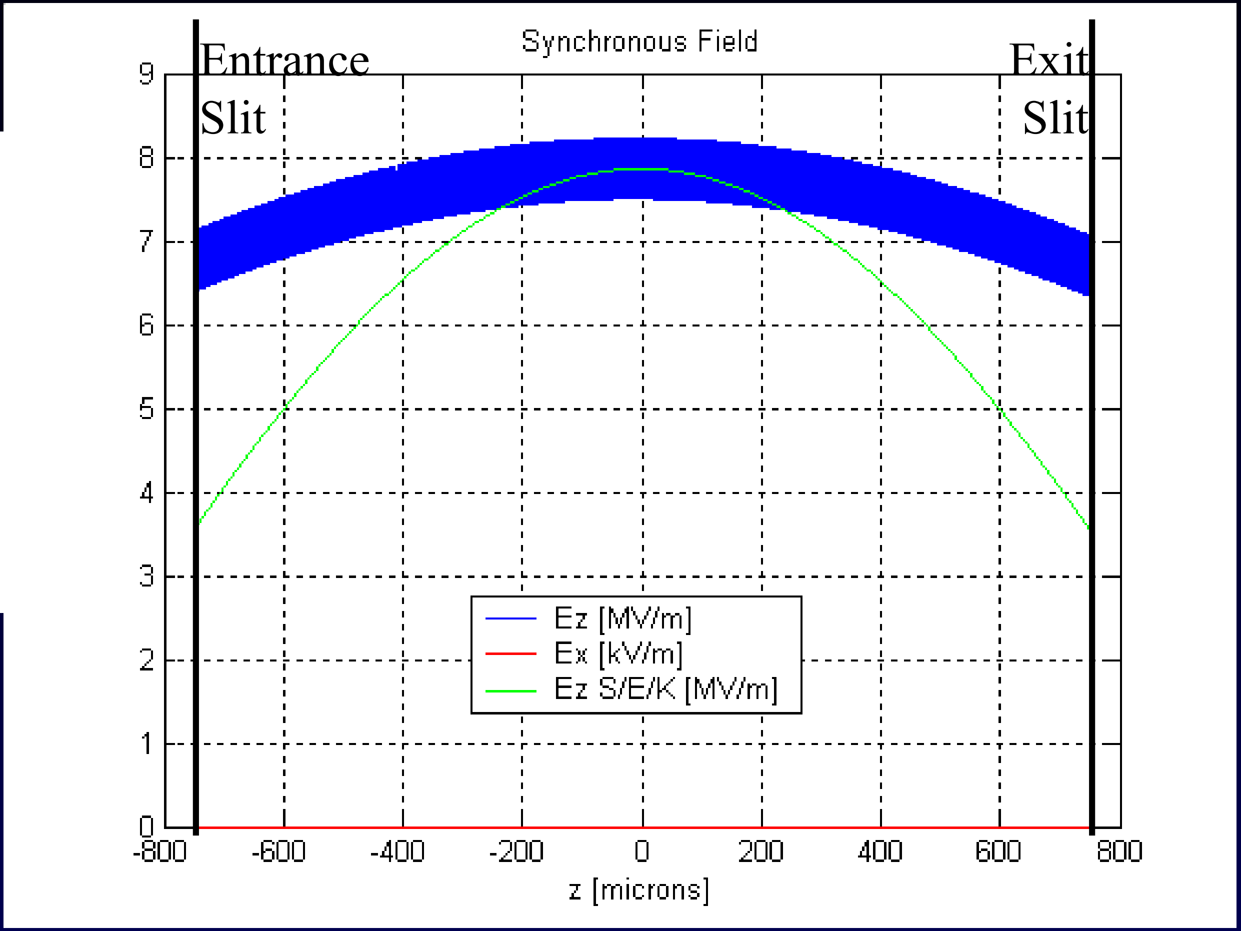

Analytic theory (Sprangle/Esarey/Krall/Ting 1996, green trace), and numerically integrated synchronous longitudinal (blue) and transverse (red) fields of crossed TEM_{00} modes. Beam slits are not accounted for in this theory.

Vector Diffraction Code

A Matlab implementation of Huygen's Principle in l.i.h. media

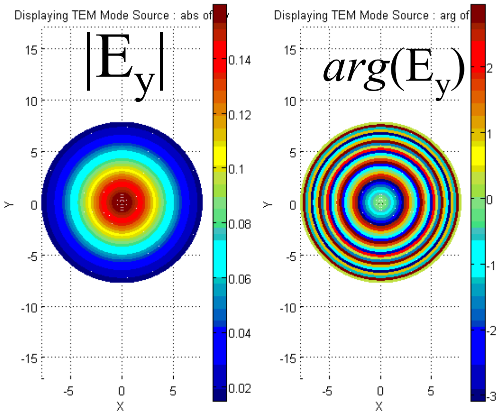

1. Construct or load incident fields

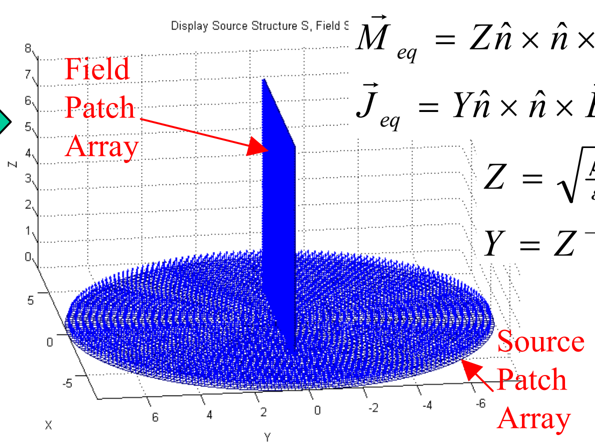

$$\vec{M}_{eq} = Z\hat{n}\times\hat{n}\times\vec{H}$$

$$\vec{J}_{eq} = Y\hat{n}\times\hat{n}\times\vec{E}$$

$$Z = \sqrt{\frac{\mu}{\varepsilon}}$$

$$Y = Z^{-1}$$

2. From incident fields, calculate surface currents on initial, discrete surface

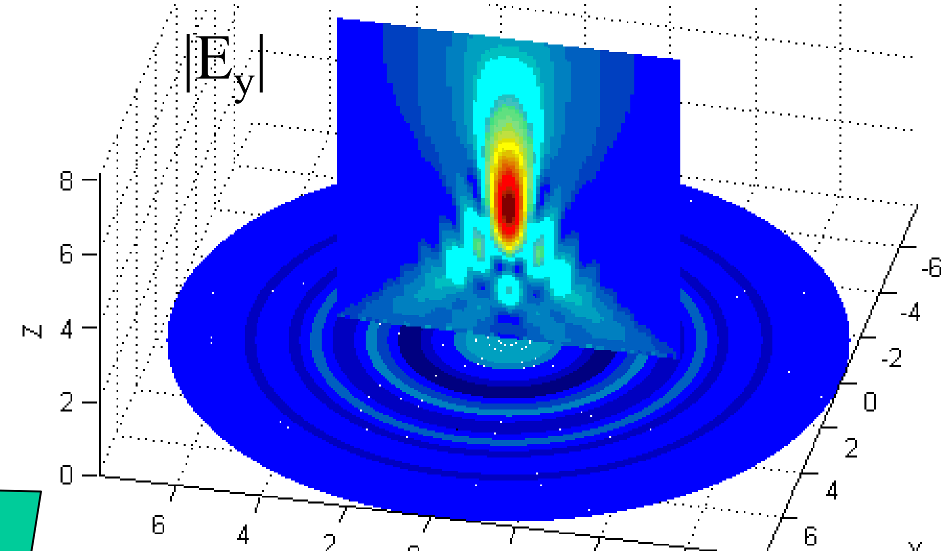

3. Propagate to field points

$$\vec{E}(r) = -\int \vec{\vec{G}}_{EJ}(\vec{R})\cdot\vec{J}(\vec{r}\,')dS' - \int \vec{\vec{G}}_{EM}(\vec{R})\cdot\vec{M}(\vec{r}\,')dS'$$

$$\vec{H}(r) = -\int \vec{\vec{G}}_{HM}(\vec{R})\cdot\vec{M}(\vec{r}\,')dS' - \int \vec{\vec{G}}_{HJ}(\vec{R})\cdot\vec{J}(\vec{r}\,')dS'$$

$$\vec{G}_{EJ}(\vec{R}) = jkZ\frac{e^{-jkR}}{4\pi R}\left[\left(\vec{1}-\hat{R}\hat{R}\right)\left(1-\frac{1}{k^2R^2}-j\frac{1}{kR}\right)+\hat{R}\hat{R}\left(\frac{2}{k^2R^2}+j\frac{2}{kR}\right)\right]$$

$$\vec{G}_{EM}(\vec{R}) = \frac{e^{-jkR}}{4\pi R}\left(\frac{1}{R}+jk\right)\hat{R}\times\vec{1}$$

$$\vec{G}_{HM}(\vec{R}) = jk_oY\frac{e^{-jkR}}{4\pi R}\left[\left(\vec{1}-\hat{R}\hat{R}\right)\left(1-\frac{1}{k^2R^2}-j\frac{1}{kR}\right)+\hat{R}\hat{R}\left(\frac{2}{k^2R^2}+j\frac{2}{kR}\right)\right]$$

$$\vec{G}_{EM}(\vec{R}) = -\frac{e^{-jkR}}{4\pi R}\left(\frac{1}{R}+jk\right)\hat{R}\times\vec{1}$$

$$\hat{R}\hat{R} = \frac{1}{R}\begin{bmatrix}(x-x')^2 & (x-x')(y-y') & (x-x')(z-z')\\(y-y')(x-x') & (y-y')^2 & (y-y')(z-z')\\(z-z')(x-x') & (z-z')(y-y') & (z-z')^2\end{bmatrix}$$

L. Diaz, T. Milligan, *Antenna Engineering Using Physical Optics*, Artech House, London, (1996).

The LEAP Cell

Analytic Theory

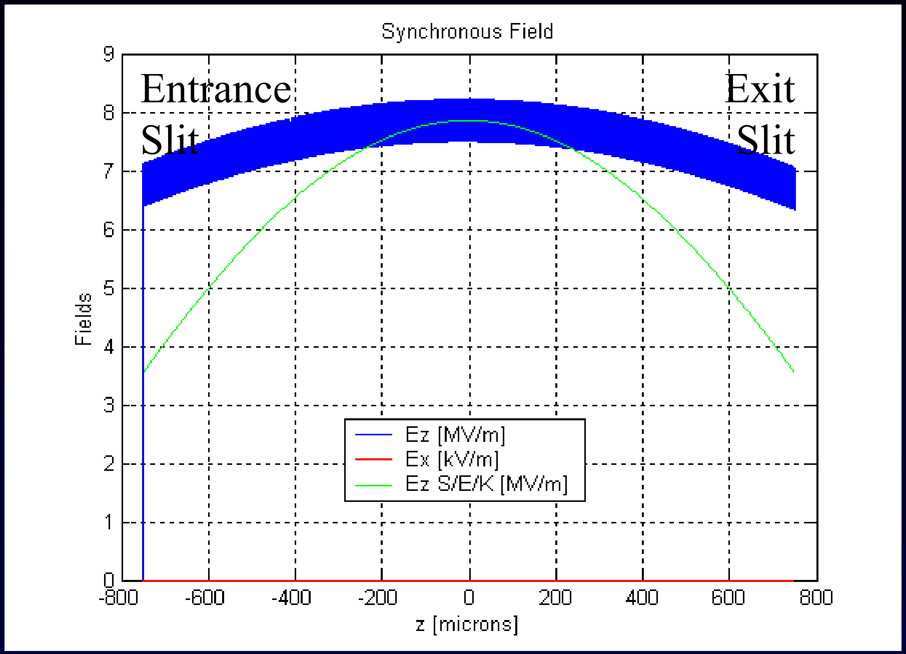

Vector Diffraction Calculation

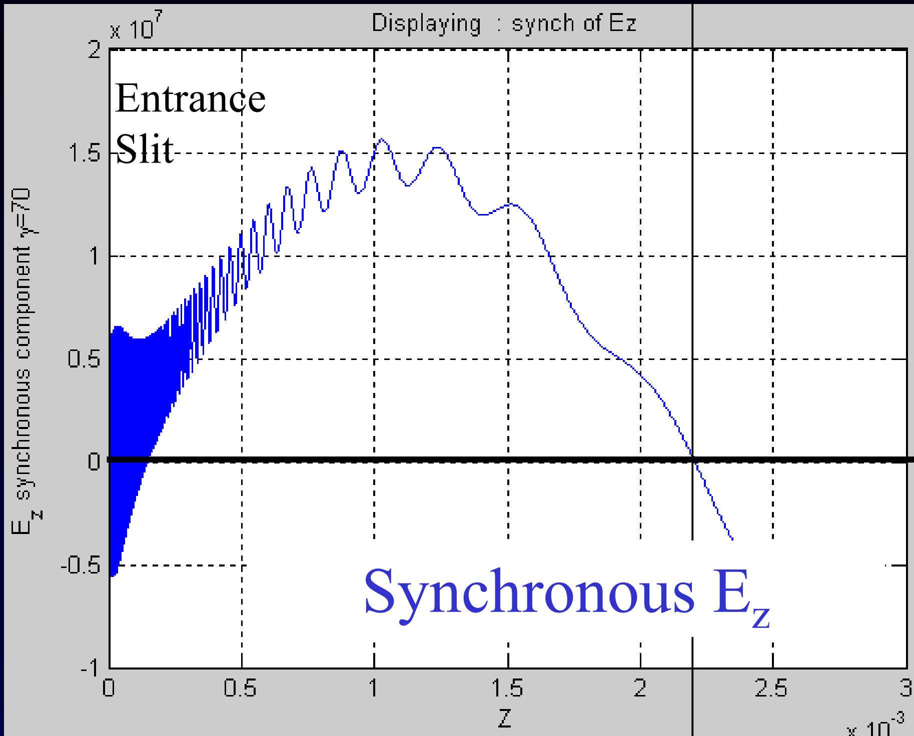

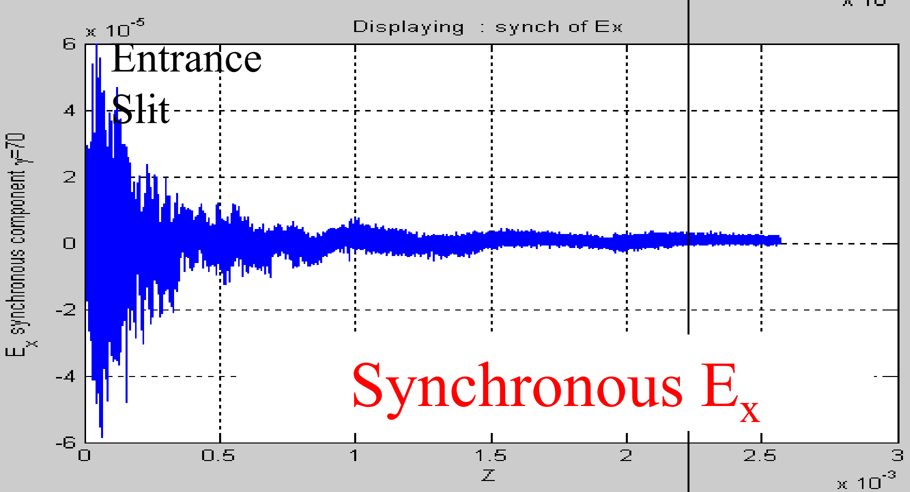

July 21, 2003

Rayleigh-Helmholtz Reciprocity Theorem (one of many reciprocity relations)

Colloquial version: Mutual inductance is reciprocal when no nonlinear media are present. (paraphrase of J. D. Kraus, *Antennas*, 2nd Ed., McGraw-Hill, New York, p.410-11, (1950), with nonlinear media clause coming from J. R. Carson, "Reciprocal Theorems in Radio Communication", *Proc. IRE*, **17**(6), p.952ff, (1929).)

Colloquial Version, Narrowly Applied to Accelerators If a structure accelerates beam, it will make the beam radiate, and the narrowband coupling impedance for each process will be the same.

Rigorous, general version: Given imposed quasistationary drive fields E_o' and E_o'' on two objects and a bounding surface S containing both objects within volume V, and ε,μ, and σ are all scalar and constant: (from S. Ballantine, *Proc. IRE*, **17**(6), p.929ff, (1929).)

$$\iiint [E_o' C'' - E_o'' C'] dv = \frac{c}{4\pi} \iint [E' \times H'' - E'' \times H']_n dS$$

$$C \equiv \tfrac{c}{4\pi} \nabla \times H$$

Original version: *"Let there be two circuits of insulated wire A and B and in their neighborhood any combination of wire circuits or solid conductors in communication with condensers. A periodic electromotive force in the circuit A will give rise to the same current in B as would be excited in A if the electromotive force operated in B."* Lord J. W. S. Rayleigh, *Theory of Sound*, v. II, Dover: New York, p. 145, (1894).

Accelerator vs. Radiator

Real(E_x)

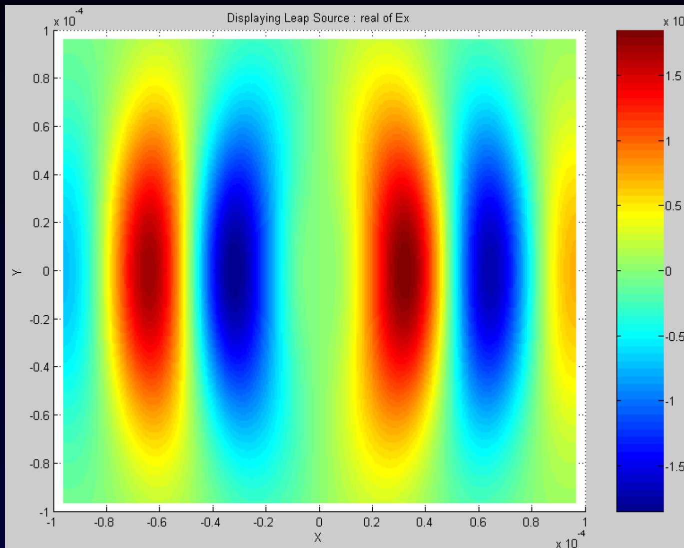

Real(E_ρ)

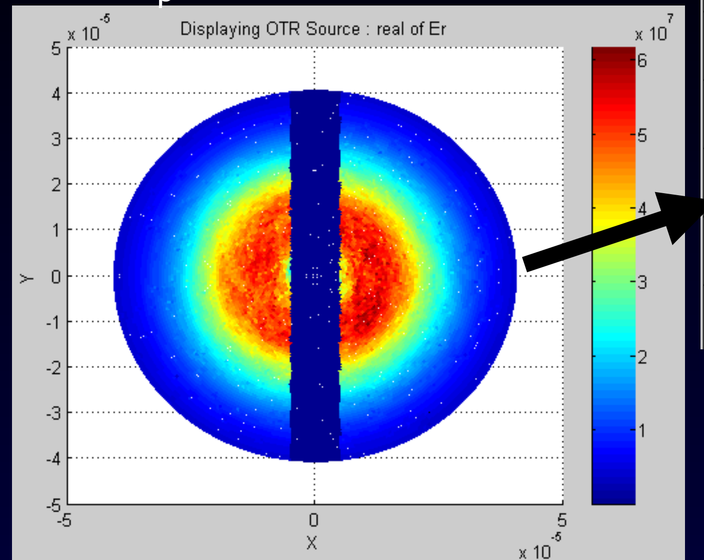

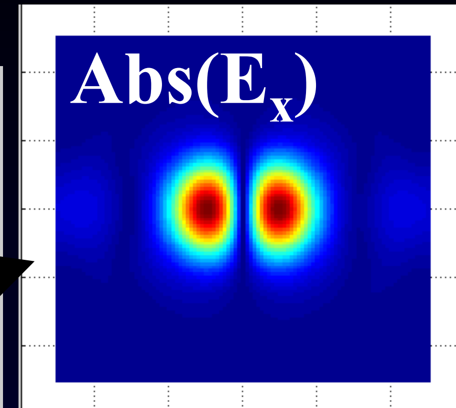

Far-field CTR
From Slit

Crossed-Beam Accelerator

Crossed Gaussian beams, w_0=64μ,

θ=11.5 mr

CTR Radiator, viewed narrowband

10μ x 10μ x λ/30 bunch, 10^4 particles

$$E_{\{x,y\}} = \sum_{i=1}^{N=10^4} \frac{e\omega}{4\pi\varepsilon_o \gamma\beta^2 c^2} \frac{\{x_i, y_i\}}{R_i} \sqrt{\frac{2}{\pi}} \exp\left(\frac{j\omega z_i}{\beta c}\right) K_1\left(\frac{R_i\omega}{\gamma\beta c}\right)$$

$$E_z = -j \sum_{i=1}^{N=10^4} \frac{e\omega}{4\pi\varepsilon_o \gamma^2\beta^2 c^2} \sqrt{\frac{2}{\pi}} \exp\left(\frac{j\omega z_i}{\beta c}\right) K_0\left(\frac{R_i\omega}{\gamma\beta c}\right)$$

$$\vec{H} \approx Y\hat{k} \times \vec{E}$$

Crossed Gaussian and ICTR give qualitatively similar accelerating fields

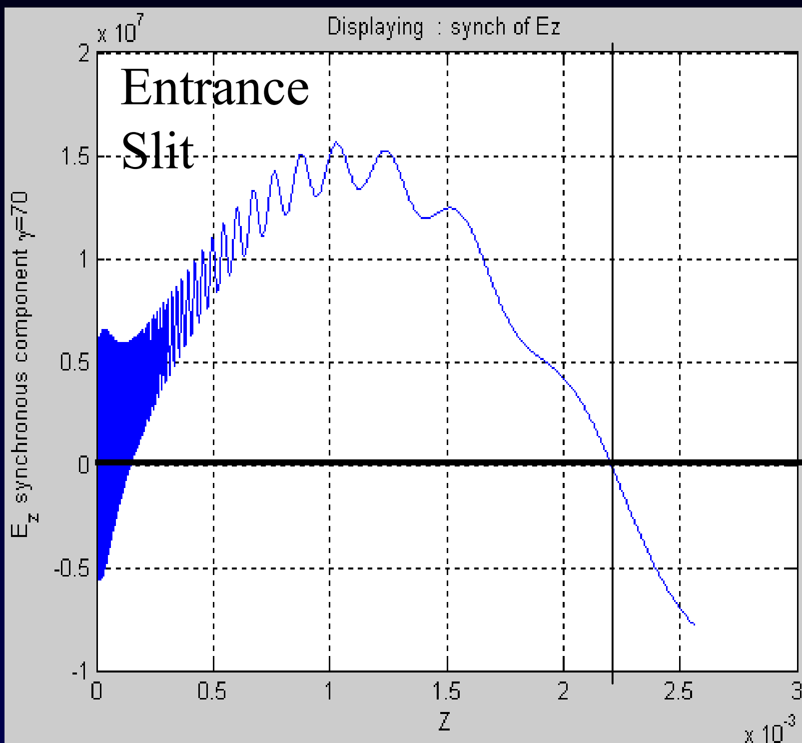

Crossed Gaussian Synchronous E_z

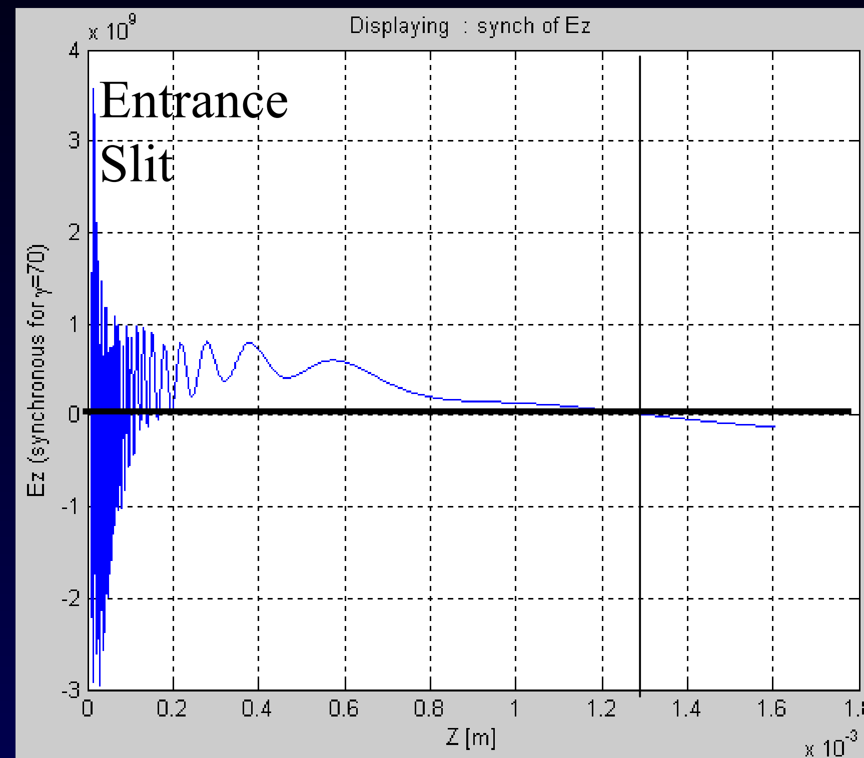

ICTR Synchronous E_z

Note: don't take vertical scales too seriously

Summary Properties

TABLE A.1: Summary of crossed-Gaussian laser and field parameters.

Parameter	**Symbol**	**Value Future**	**Value Now**	**Comment**
Electron Energy	E_e	60 MeV	60 MeV	
Laser Wavelength	λ	0.8 μm	0.8 μm	
Laser focal spot size	w_o	50 λ	50 λ	
Rayleigh Range	z_R	6.3 mm	6.3 mm	
Slippage Length	z_s	2.8 mm	2.8 mm	
Ideal Crossing Angle	θ	11.5 mrad	11.5 mrad	$1/\gamma$=8.3 mrad
Critical Energy	γ_c	68	68	(34 MeV)
Spot size on dielectric surface	w_1	51.3 λ	51.3 λ	
Fluence x time on dielectric surface	$F \cdot \Gamma_t$	2 J/cm^2	0.5 J/cm^2	
Laser Pulse Energy	E_γ	100 μJ	25 μJ	
Laser Pulse Length	Γ_t	100 fsec	5 psec	FWHM
Peak Electric Field	E_o	5.9 GV/m	0.42 GV/m	
Peak Axial Field	E_z	140 MV/m	9.8 MV/m	
Energy Gain	ΔW	290 keV	20 keV	Ideal phase particle
Electron Beam Energy Spread	Γ_E	20 keV	20 keV	FWHM

But it should be noted that $Z'=3\times10^{-4}\ \Omega/\lambda$!

Second Example: Photonic Band Gap Structures

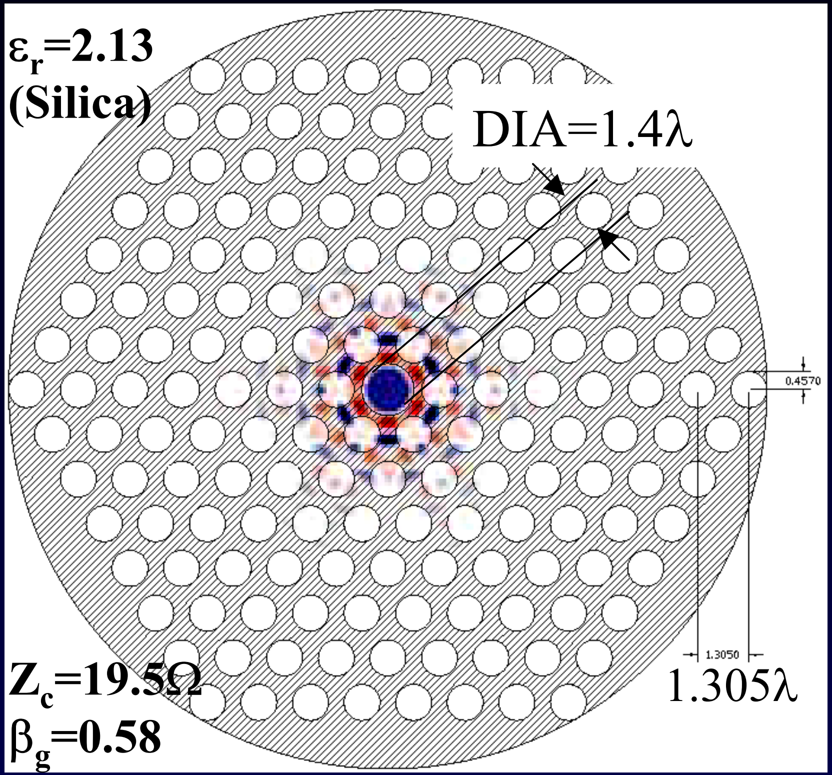

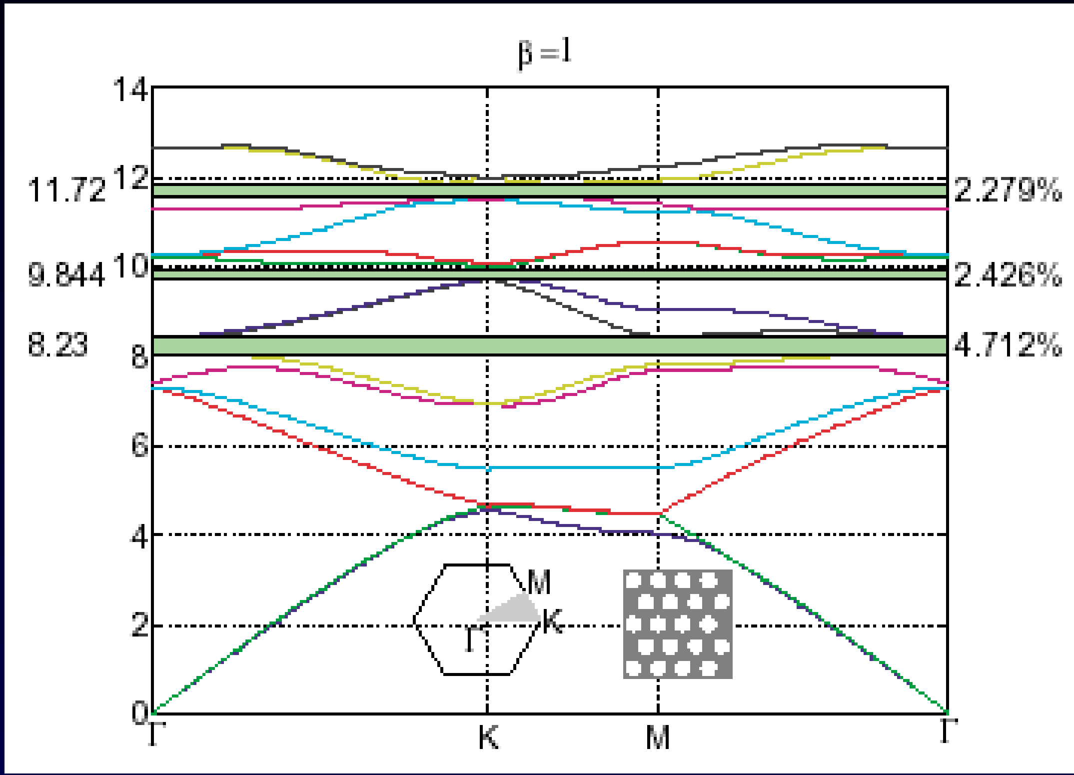

X. (Eddie) Lin, "Photonic Band Gap Fiber Accelerator", *Phys. Rev. ST-AB*, **4**, 051301, (2001).

- Can be designed to support a single, confined, synchronous mode
- All other modes at all other frequencies radiate strongly

$$Z_c = \frac{|E_{\text{acc}}|^2 \lambda^2}{2P}$$

2D Photonic Band Gap Structures

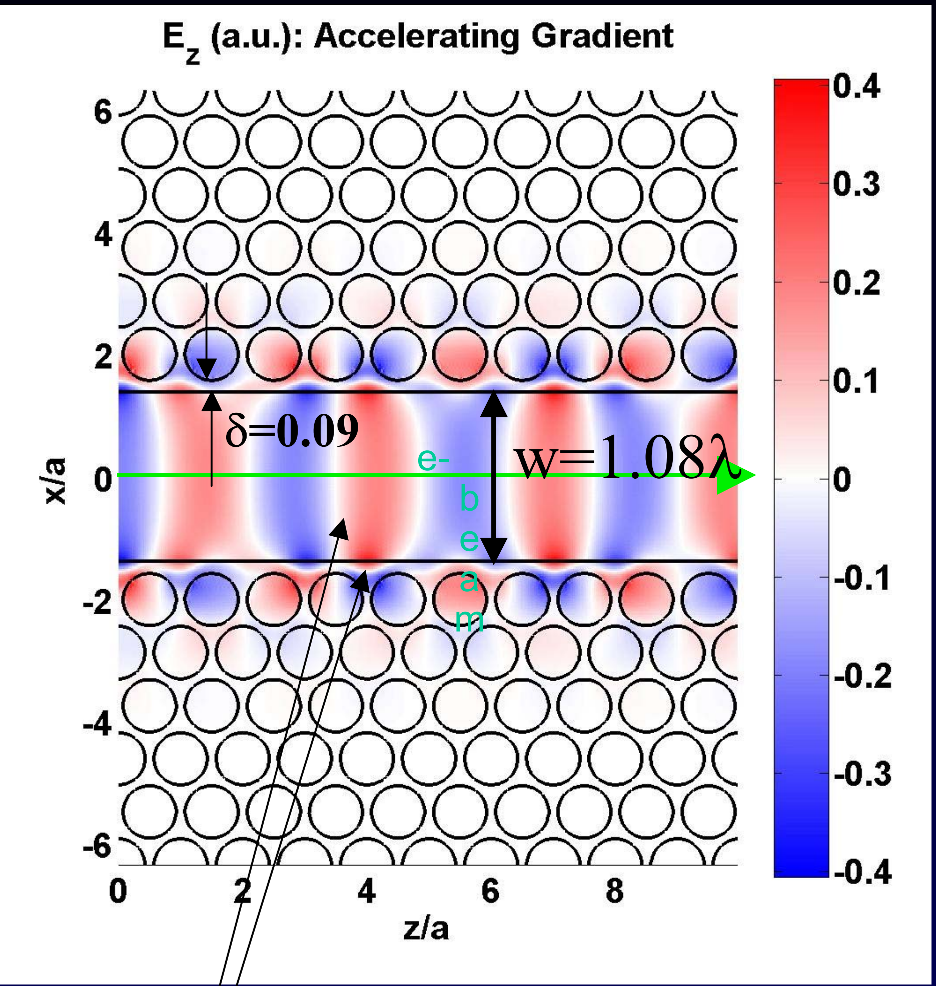

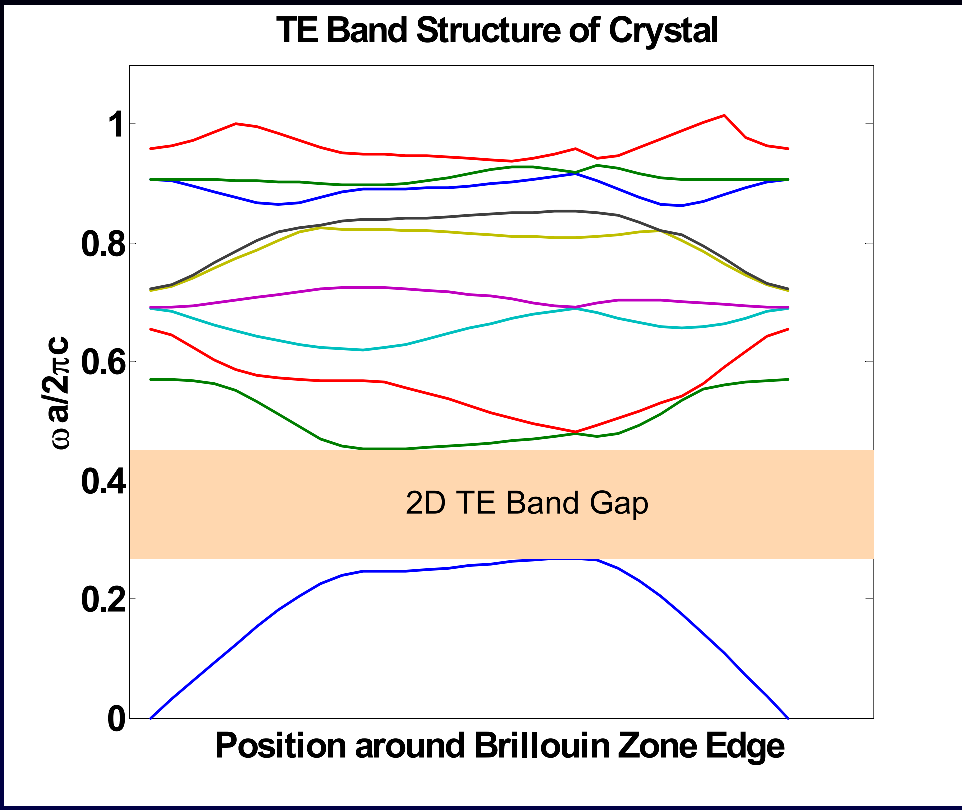

$a=0.36\lambda$

$\varepsilon_r=12.1$
(Silicon)

This geometry is designed for the lithographic process.

Ben Cowan, ARDB, SLAC

Impedance and Gradient Optimization

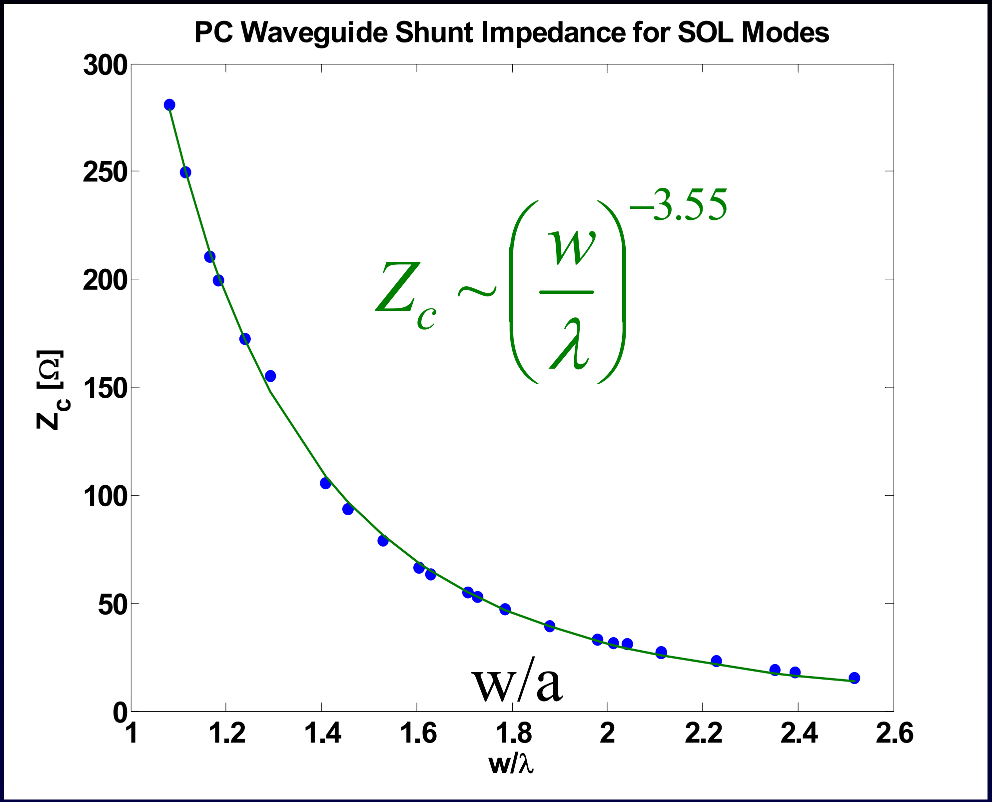

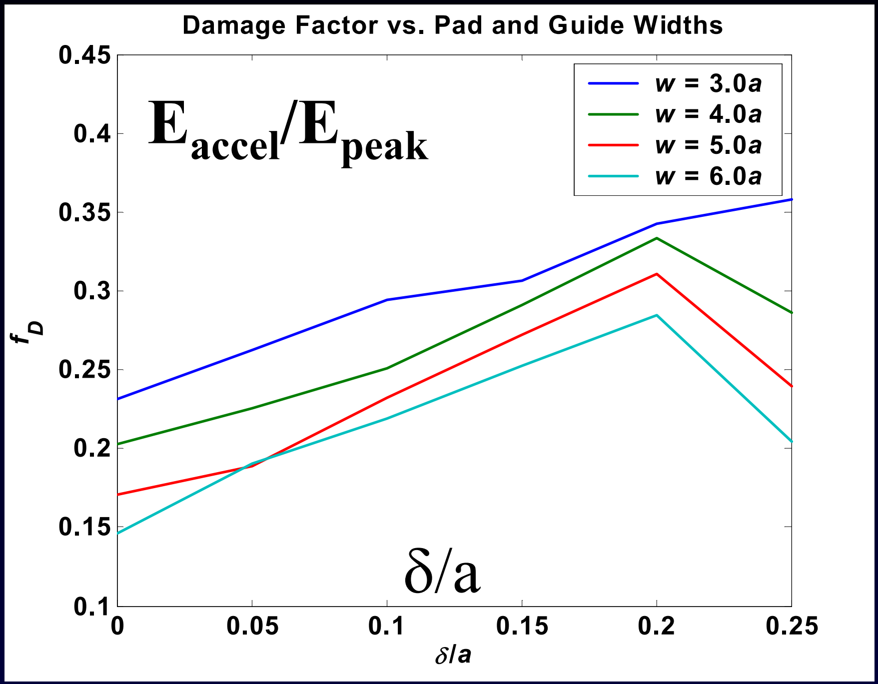

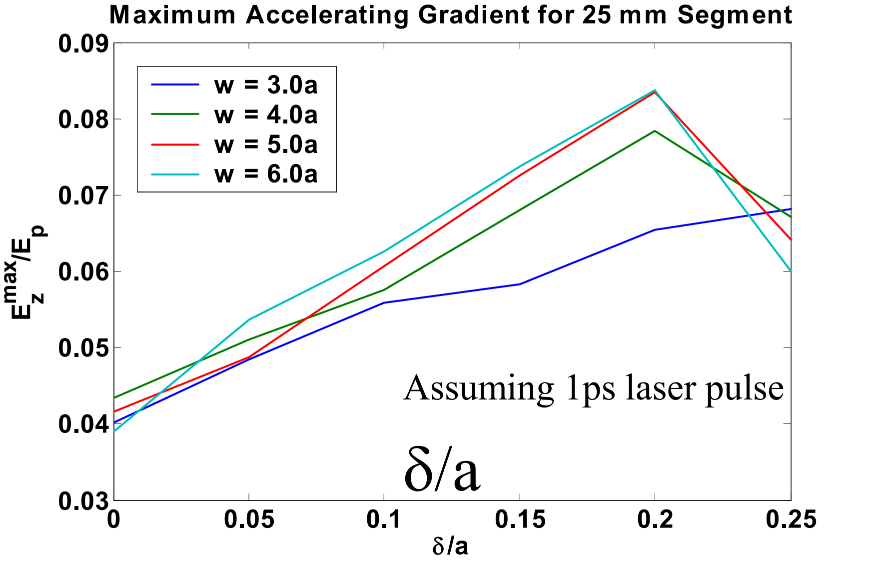

Ben Cowan, ARDB, SLAC

July 21, 2003

2D Fiber Structures

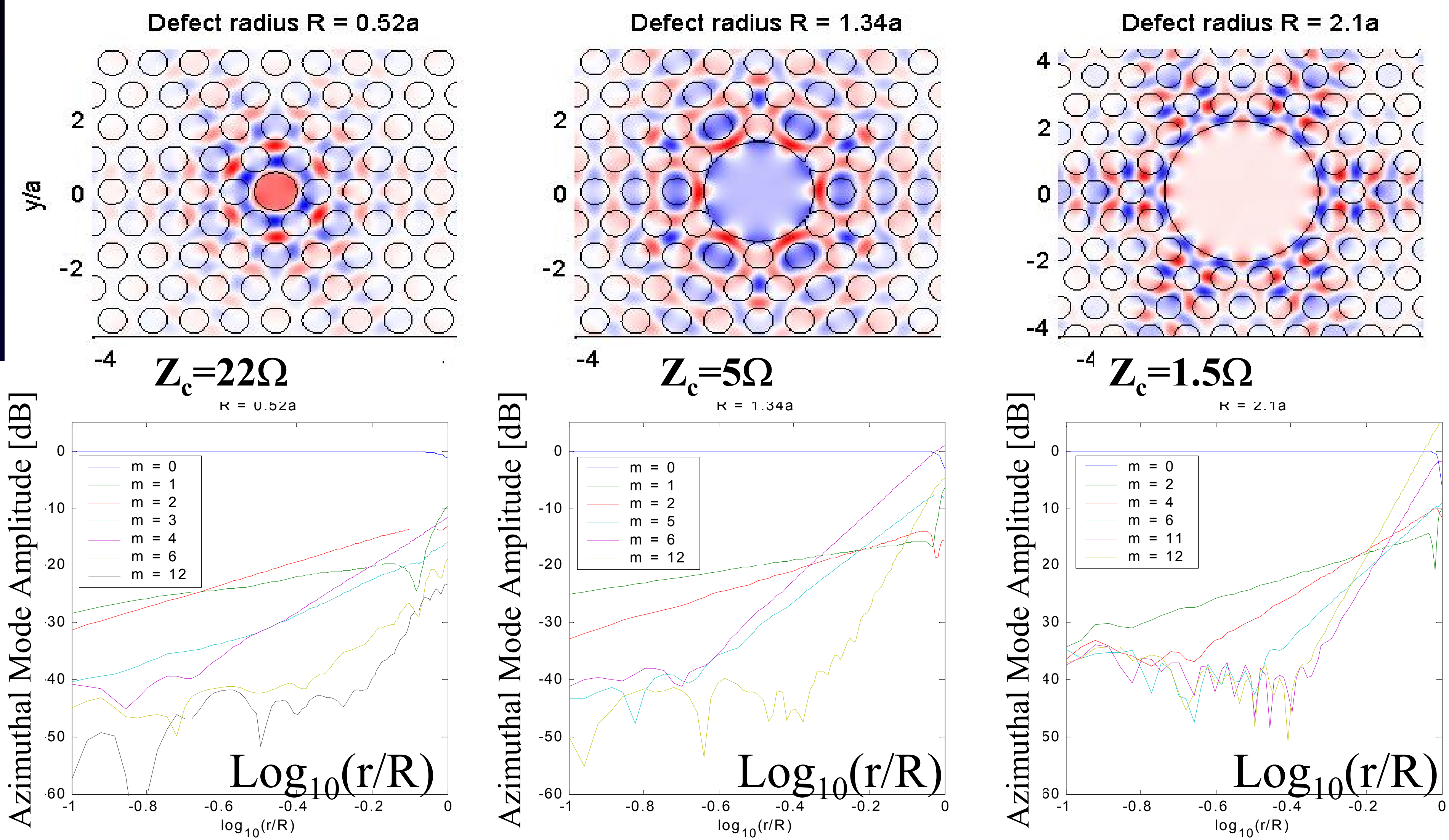

This geometry is designed for the fiber drawing process.

Fabricated Examples

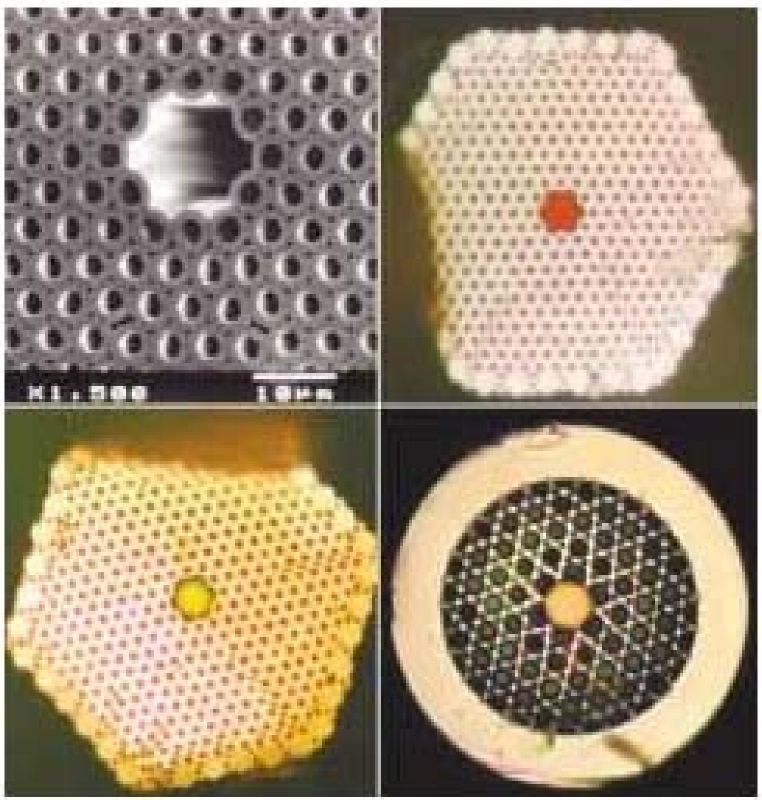

P. Russell, “Holey fiber concept spawns optical-fiber rennaissance”, *Laser Focus World,* Sept. 2002, p. 77-82.

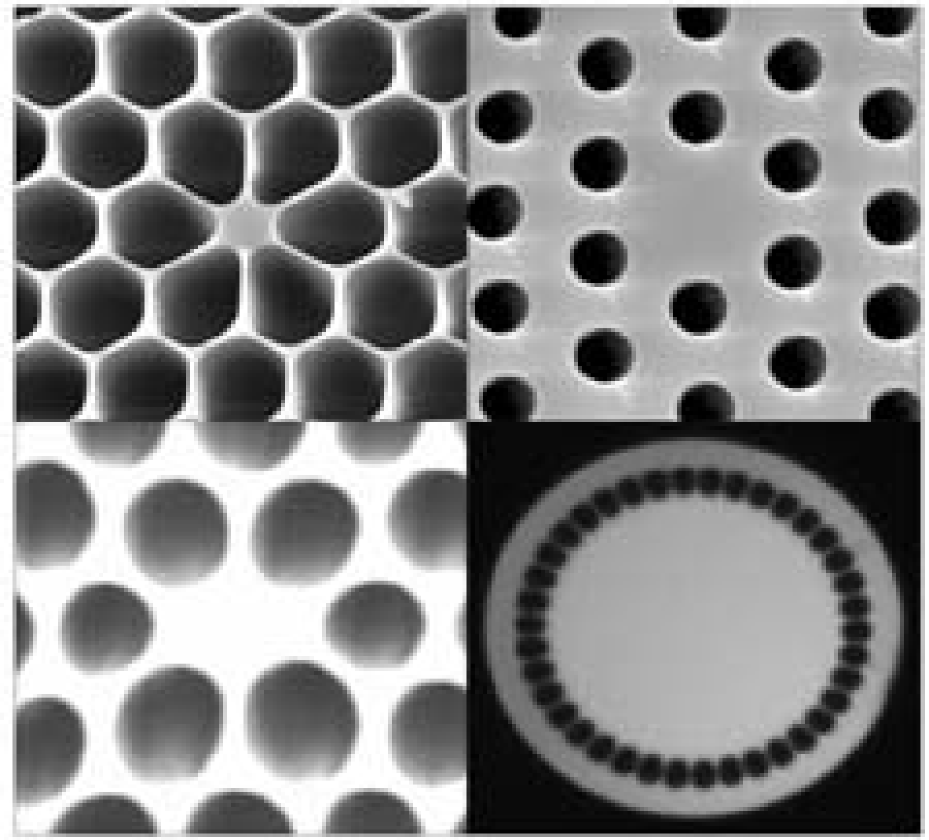

PCF structures vary according to application: (a) highly nonlinear fiber; (b) endlessly single-mode fiber; (c) polarization maintaining fiber; (d) high NA fiber. From René Engel Kristiansen (Crystal Fibre A/S), “Guiding Light with Holey Fibers,” *OE Magazine* June 2002, p. 25.

Hollow Fiber Bragg Accelerator

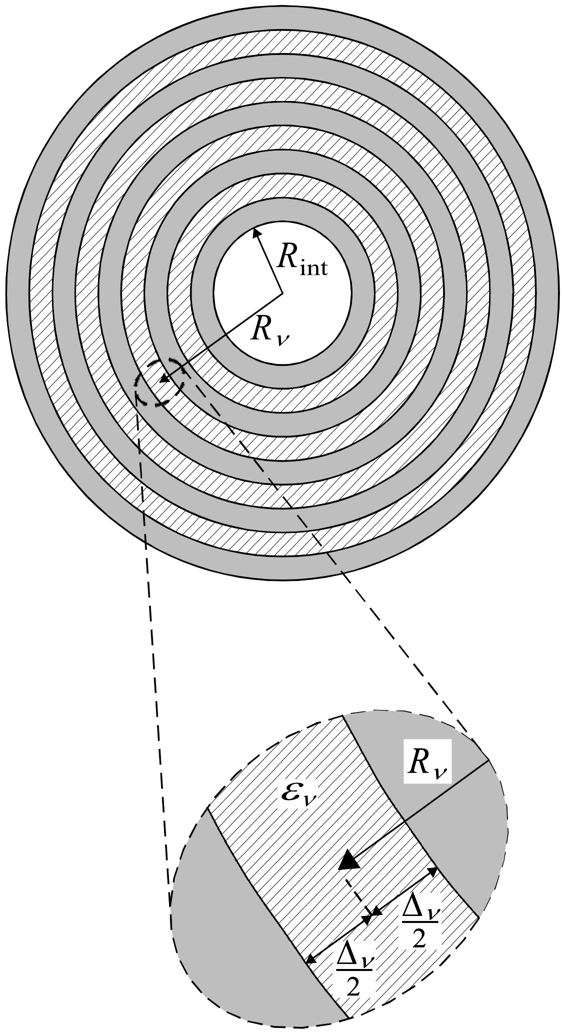

\# Concentric layers ($\varepsilon_1,\varepsilon_2$)

\# Each layer □ $\lambda / 4\sqrt{\varepsilon - 1}$

\# $v_{ph} = c$

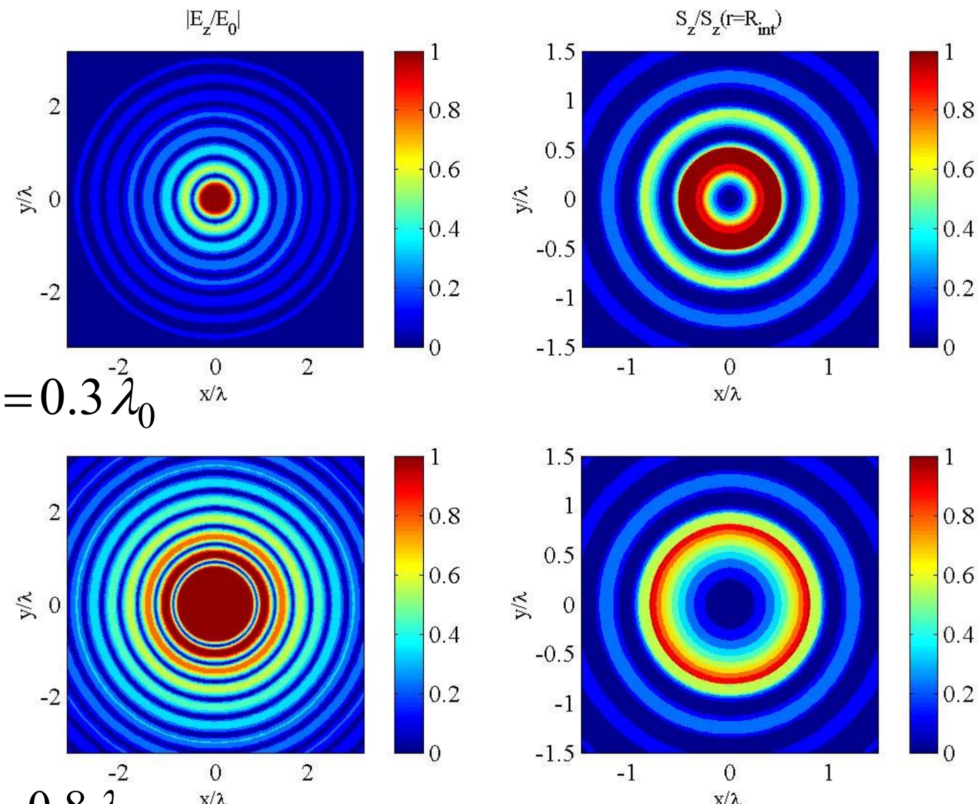

$R_{\text{int}} = 0.3\,\lambda_0$

$R_{\text{int}} = 0.8\,\lambda_0$

Levi Schächter, The Technion

Towards a Laser Linear Collider

Emittance and Beam Transport

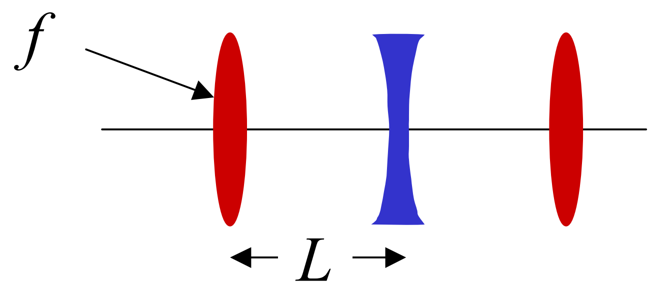

If a is the beam hole radius, the acceptance is

$$A = \frac{a^2}{\beta_{\max}} = n\frac{\varepsilon_I}{\gamma}$$

$n \equiv$ clearance $= 25$ for 5σ beam

$\varphi \equiv$ phase advance/half-cell

$$\beta_{\max} = 2f\frac{1+\sin\varphi}{\cos\varphi}$$

$$f = \frac{\gamma mc}{eGl}$$

For a quad of length l and gradient G

$$\varepsilon_I = \frac{a^2}{n}\frac{eGl}{2mc}\frac{\cos\varphi}{1+\sin\varphi}$$

Example

$$G = 2.5kT/m; l = 1.0cm; \gamma = 2\times 10^4 \Rightarrow f = 1.36m$$

$$\varphi = 45^o \Rightarrow L = 1.93m$$

$$a = 1.2\lambda = 2.4\mu m; n = 25 \Rightarrow \boxed{\varepsilon_I = 7\times 10^{-4}\pi \text{ mm-mr}}$$

R. Siemann, ARDB

Injector Concept

While $\varepsilon_N = 7\times10^{-4}\ \pi$ mm-mr is a very small emittance, the phase space density $Q/\varepsilon_N = 5\times10^5 e / 7\times10^{-4} = 0.12$ nC/mm-mr, an order of magnitude lower than the phase space densities demonstrated by rf photoinjectors now.

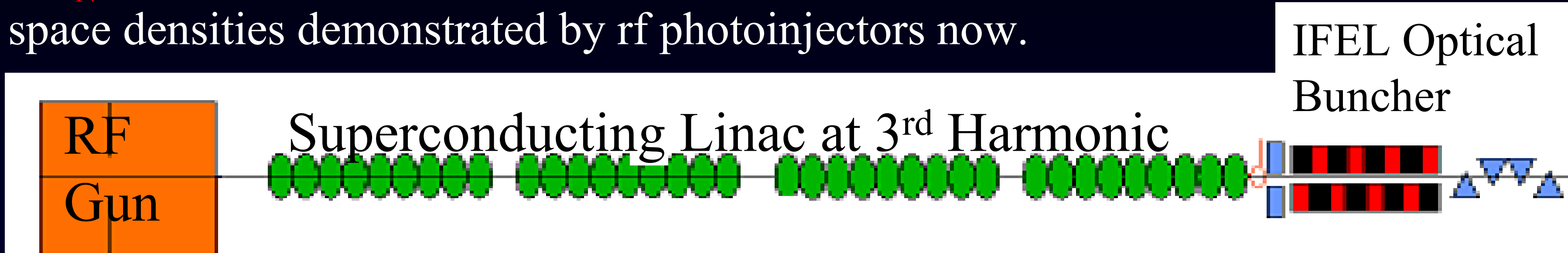

Laser Linear Collider Injector Parameters		
Gun		
Photocathode	CsTe	
Quantum Efficiency	1%	
Structure	1.6 cell room-temperature gun	
Frequency	433 MHz	
Duty Cycle	100%	
Solenoid	20cm x 1 kG, mounted over gun	
Laser Properties		
Laser Pulse Energy (UV)	47 pJ	
Average Laser Power (UV)	20 mW	
Average Laser Power (IR)	0.2 W	10% IR-->UV
Spot Diameter at Cathode	1.1 µm	Flat-top
Laser Pulse Length	20 ps FWHM	Flat-top

Accelerator	
Structures	TESLA 9-cell Niobium Cavity
Number of Sections	4
Frequency	1300 MHz
Accelerating Gradient	18 MeV/m
Bunch Properties	
Bunch Charge	5.77x10^5 electron per pulse
Energy at gun exit	7.5 MeV
Energy at accelerator exit	61.5 MeV
Bunch Emittances	7.7x10^-4 pi mm-mr
	7.7x10^-4 pi mm-mr
	70 pi deg-keV
Bunch Length	7.7 ps rms
Energy Spread	92 keV
Bunch Density (Q/emittance)	0.12 nC/mm-mr
(LCLS	1.00 nC/mm-mr)

First pass PARMELA simulations show this emittance is not unreasonable.

First-Pass Luminosity Calculation

$$P_b = (nN) f_r \gamma mc^2$$

$$N_\gamma = 2.12 \frac{\alpha r_e (nN)}{\sigma_x + \sigma_y}$$

$$L \propto \frac{N_\gamma P_b}{\gamma \sigma_y (1 + \sigma_y / \sigma_x)}$$

$$\xi_1 = \frac{2 r_e^2 N \gamma}{\alpha \sigma_z (\sigma_x + \sigma_y)}$$

E_{CM} = 500 GeV	**Laser**	**JLC/NLC**
N	5×10^6	9.5×10^9
f_c	50MHz	11.4kHz
P_b (MW)	10	4.5
σ_x/σ_y (nm)	0.5/0.5	330/5
N_γ	0.22	1.1
σ_z (μm)	120	300
σ_z/c (psec)	0.4	1
ξ_1	0.045	0.11
$\boldsymbol{L}$	$\mathbf{1\times10^{34}}$	$\mathbf{5.1\times10^{33}}$

•Optical bunching within the short macropulses must be destroyed, otherwise beamstrahlung is unacceptably high. Can do this after acceleration with small R_{56}.

Laser Linear Collider Cartoon

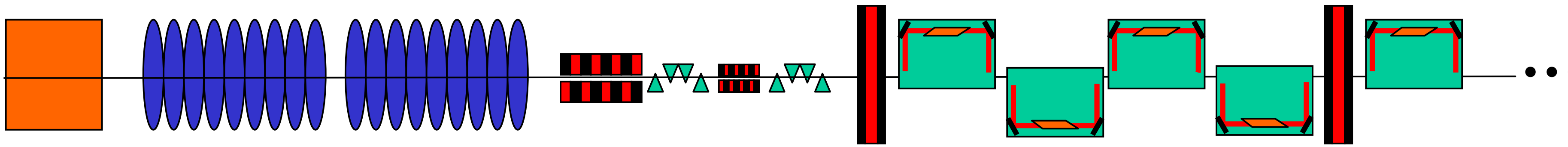

CW Injector

Warm rf gun   Cold Preaccelerator   Optical Buncher

433 MHz x 5E05 e^-/macropulse (600 μpulse/macropulse)

$\varepsilon_N \sim 10^{-11}$ m (but note $Q/\varepsilon_N \sim 1$ μm/nC)

Laser Accelerator

λ=1-2 μ, G~1 GeV/m

Photonic Band Gap Fiber structures embedded in optical resonant rings

Permanent Magnet Quads (B'~2.5 kT/m)

An Acceleration Unit

Resonant ring path length: λ_{rf}=23 cm

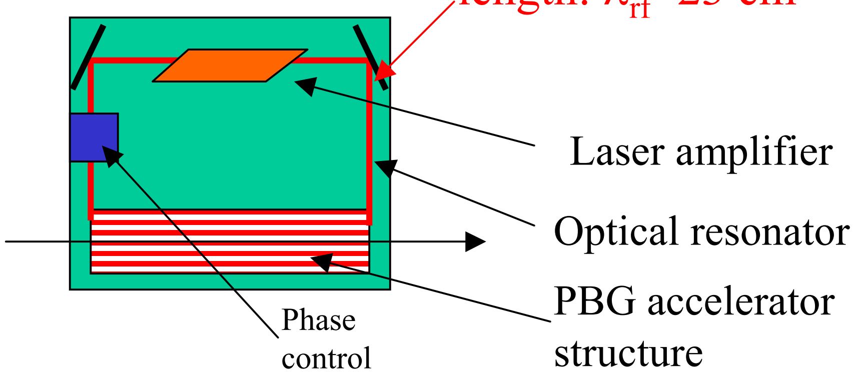

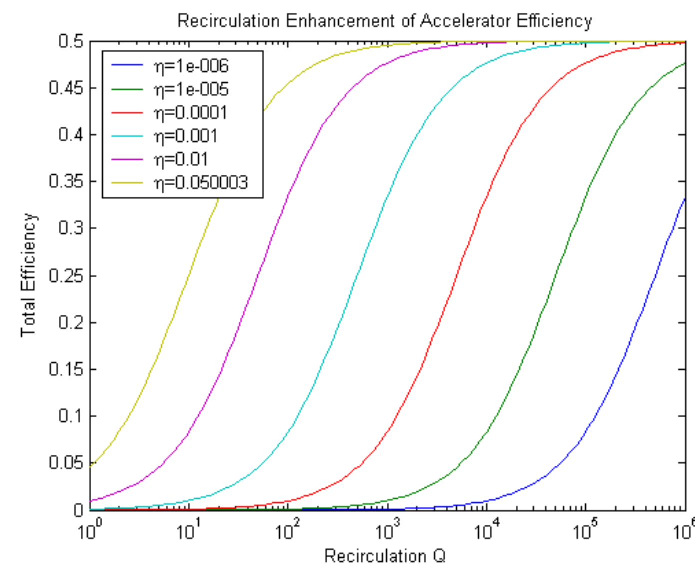

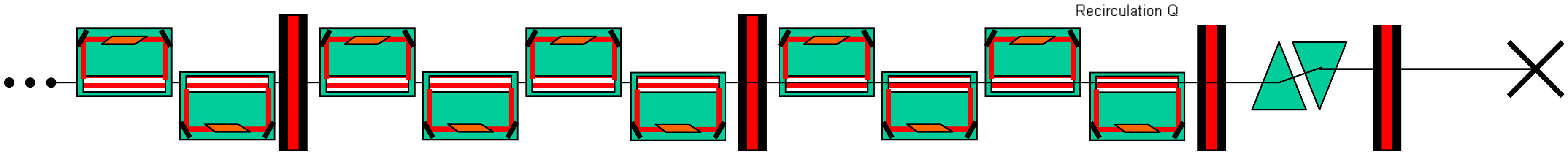

Optical Debuncher   **Final Focus**   **I.P.**

Experimental Efforts in Vacuum Laser Acceleration

The Inverse Free Electron Laser

STELLA (Staged Electron Laser Acceleration) experiment at the BNL ATF

(STI Optronics/Brookhaven/Stanford/U. Washington)

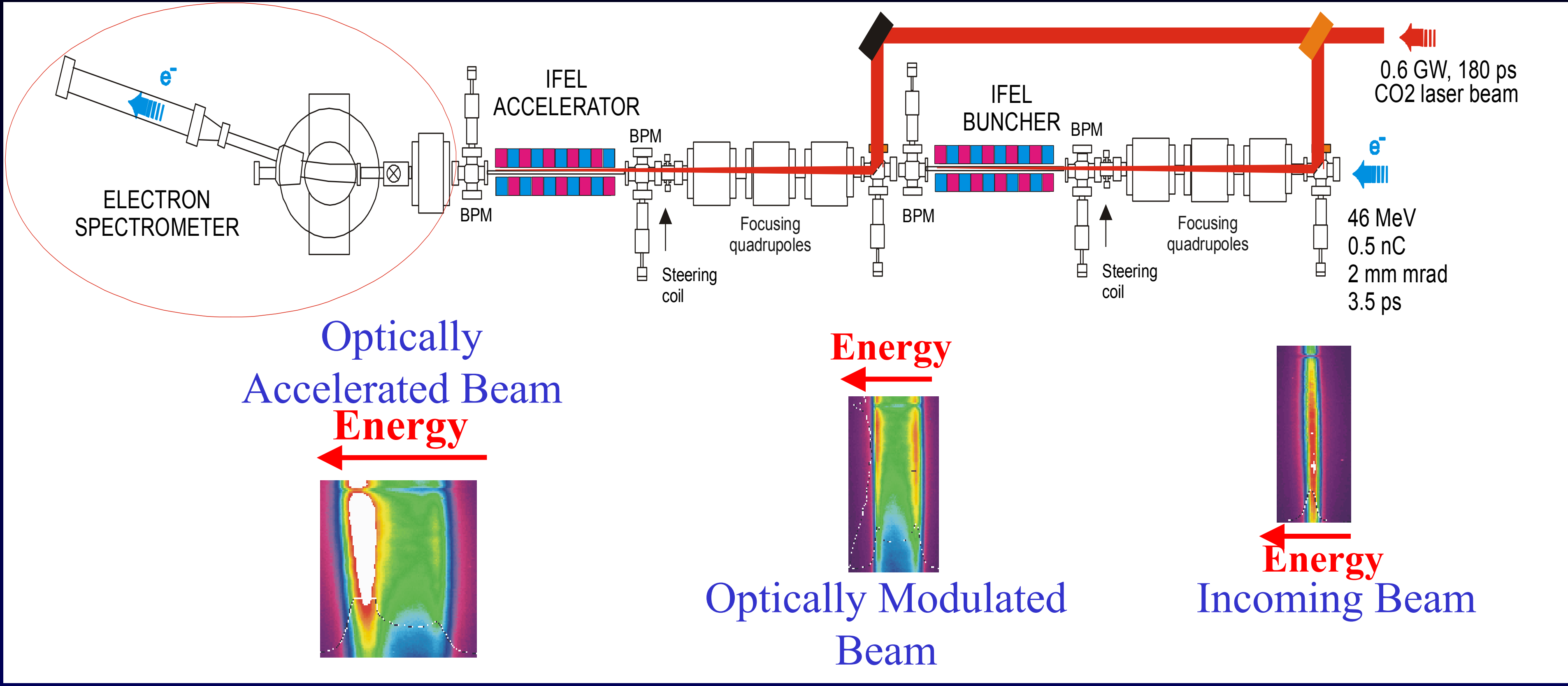

W. Kimura, I. Ben-Zvi, in proc. of Adv. Accel. Conc. Conf., Santa Fe, NM, 2000.

Multicell Linear Acceleration Experiments

Multiple ITR Accelerators
Y.-C. Huang, NTHU, Taiwan
(at Brookhaven)

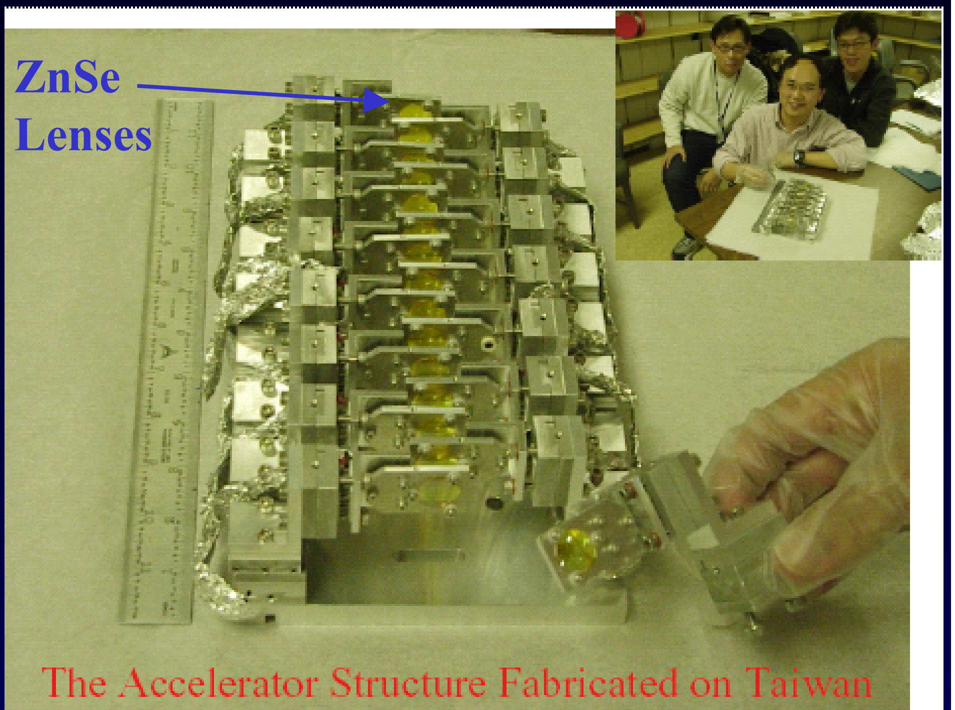

Expected gain: 250 keV over 24cm.

Y-C. Huang, *et al*, Nat'l Tsinghua University. Images from ATF User's Meeting, January 31, 2002.

Inverse Cerenkov Acceleration in Waveguide
(Unfolded Fabry-Perot Interferometer)
A. Melissinos, R. Tikhoplav (U. Rochester, Fermilab)

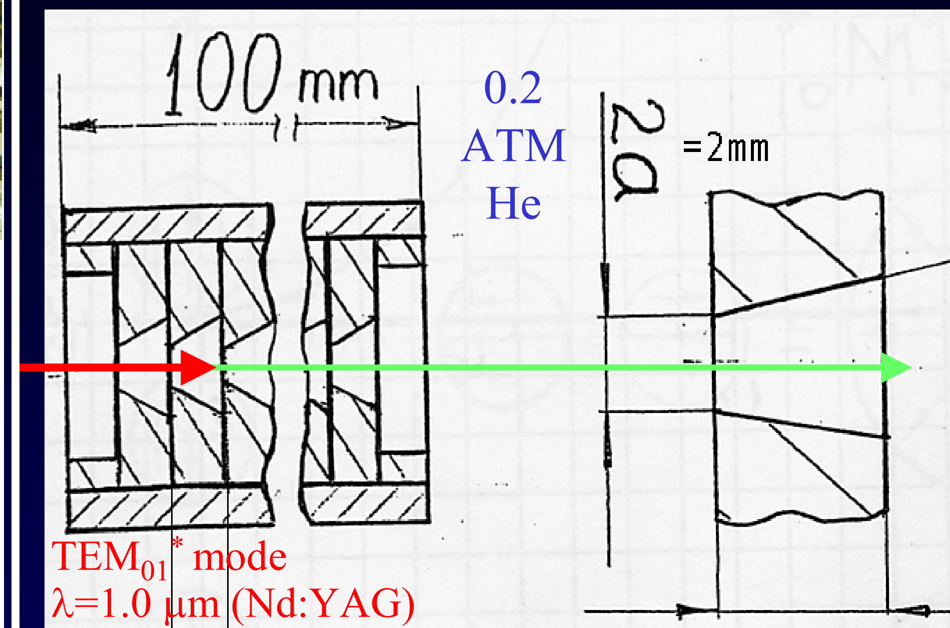

Status: Structure has been fabricated with 80% power transmission measured. Nd:YAG drive laser is under construction at Fermilab now.

The LEAP Accelerator Cell

"Laser Electron Acceleration Project"

Stanford University (Appl Phys. & HEPL) / SLAC

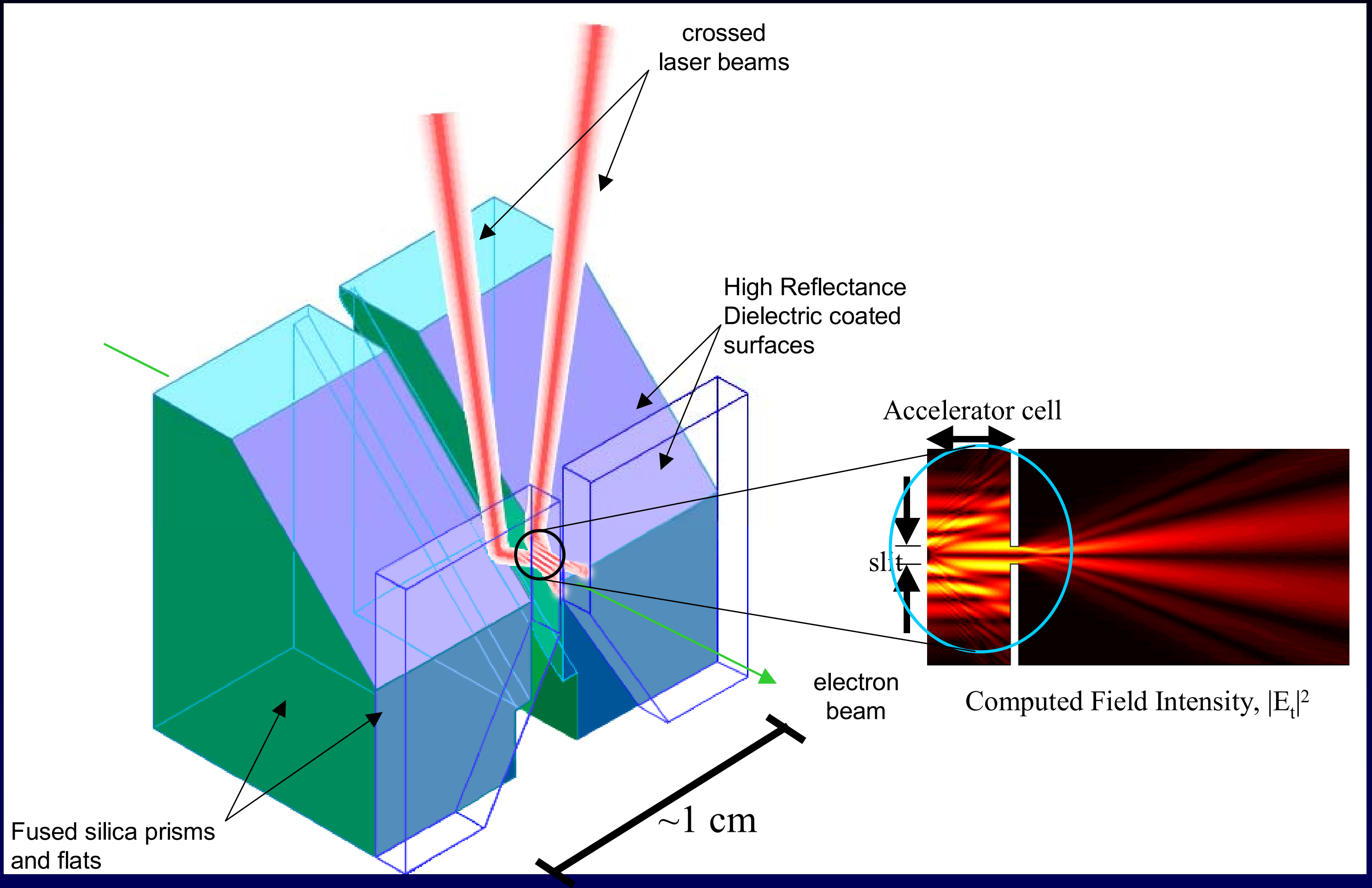

The LEAP Accelerator Cell

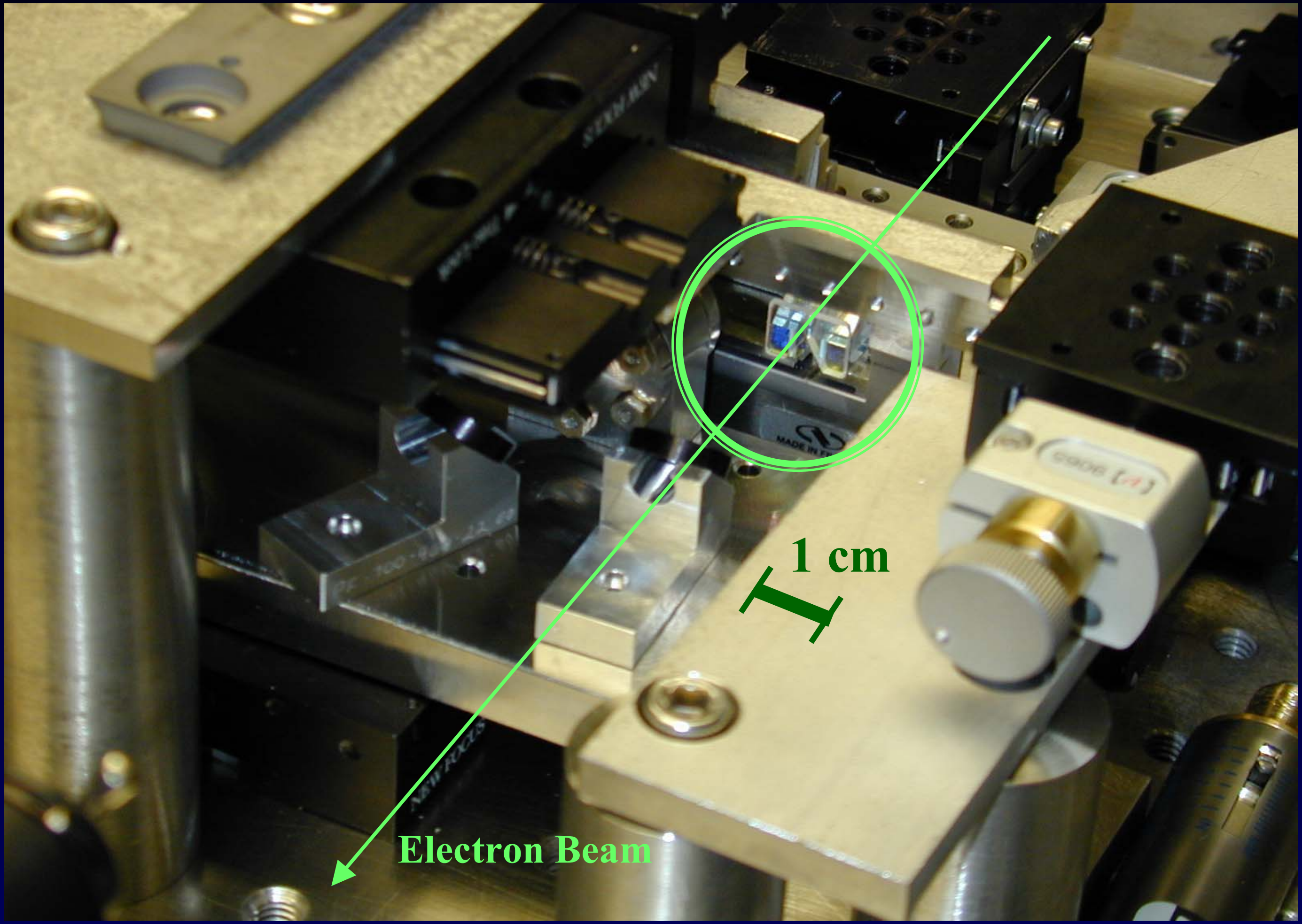

The LEAP Experimental Setup

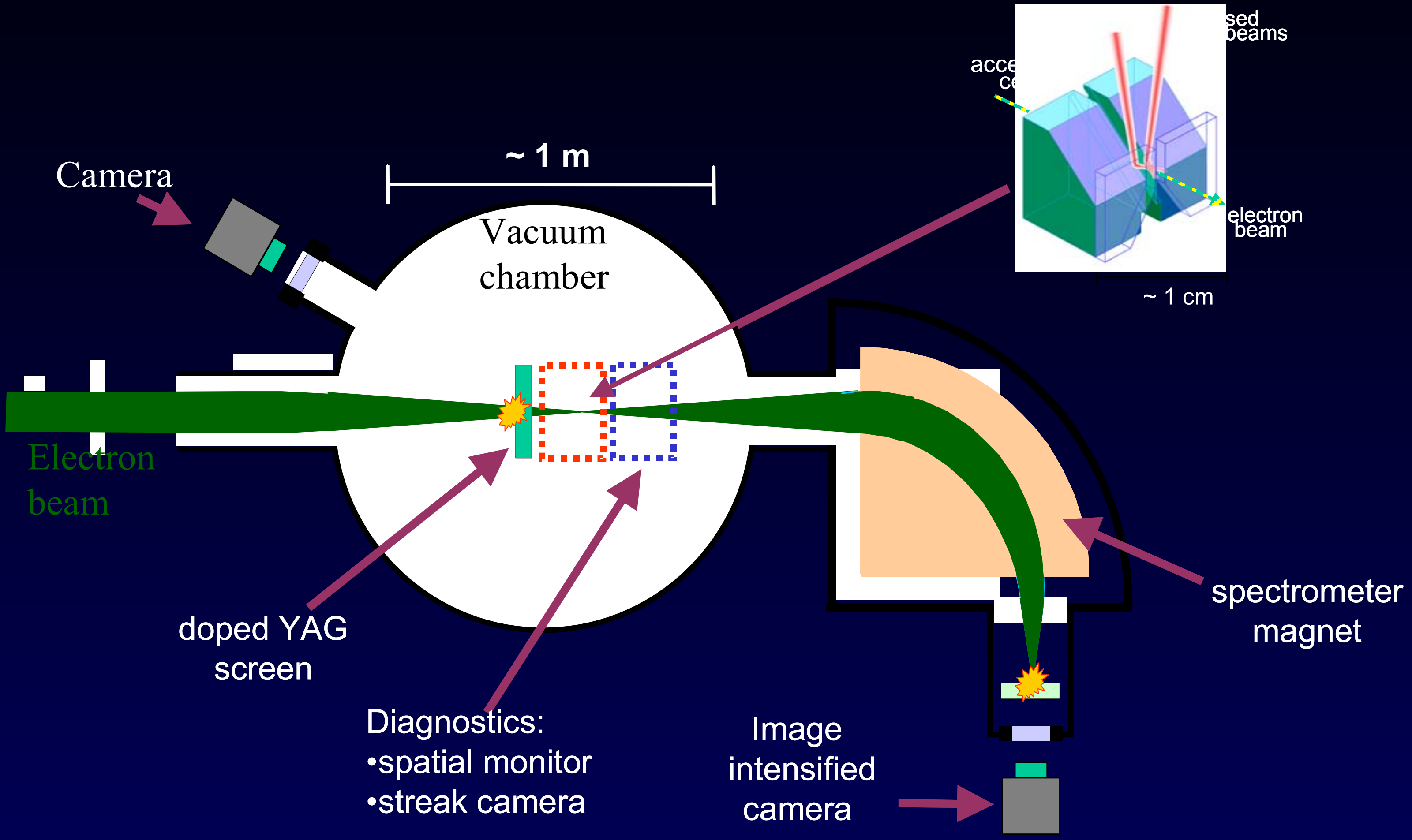

Precision Low-Charge Spectrometry

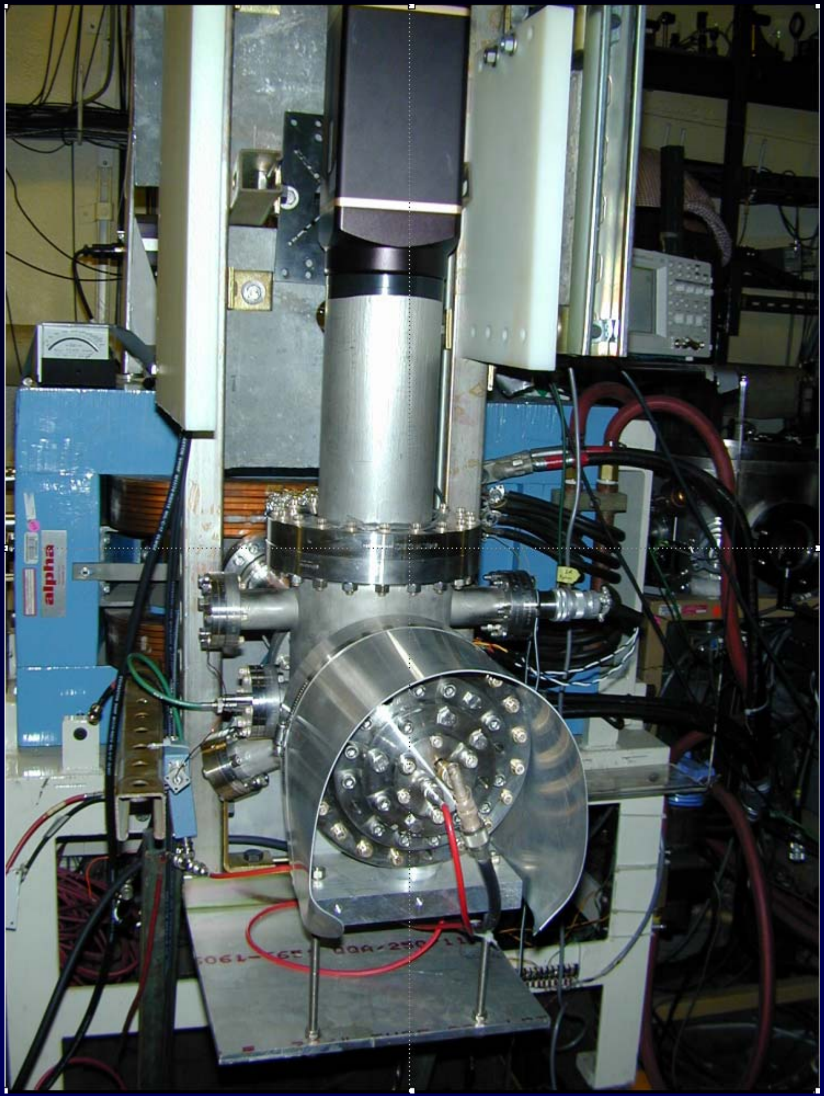

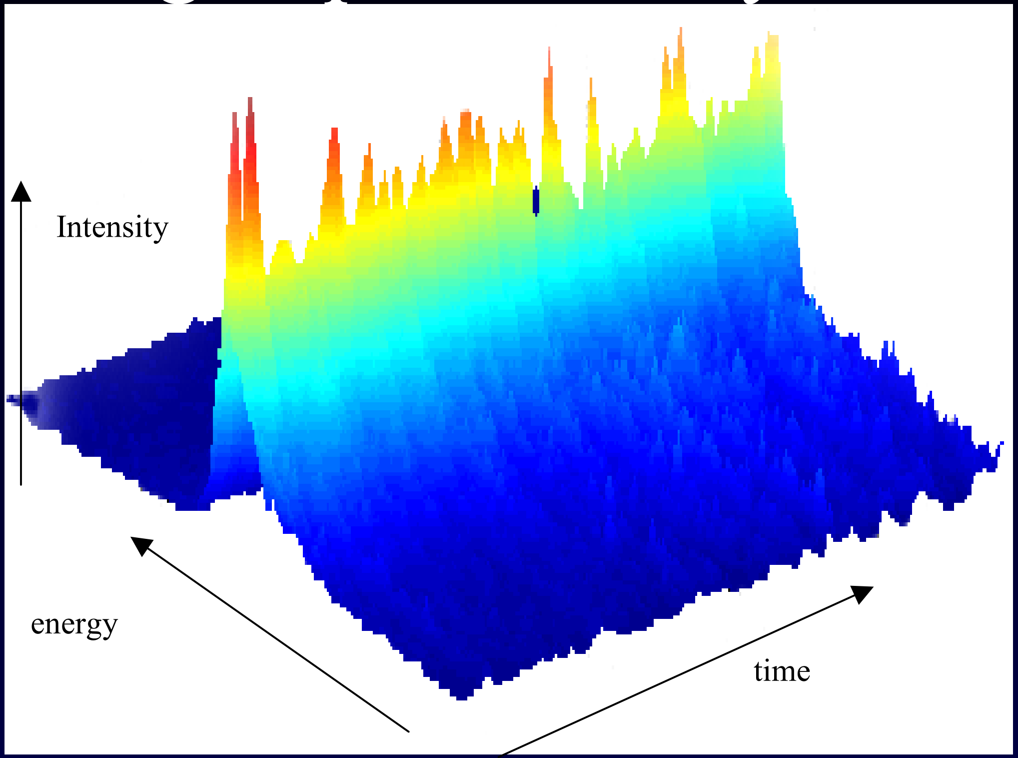

2 keV (1:10^4) resolution spectrometry with sub-picoCoulomb beams

Ce:YAG scintillator, ICCD

Timing Diagnostics

Three separate systems used, depending on circumstances

1. Coarse Timing (~1 nanosecond scale)
   PMT watches for bremstrahlung xrays from the beam
   Photodiode watches the laser
   → signals summed and transmitted on common cable; scope observation

2. Fine Timing (~5 picosecond resolution; relative, nondestructive)
   Rf cavity samples 11.8 MHz beam at 238th harmonic (2.812 GHz)
   Photodiode observes laser (82.7 MHz), generate 34th harmonic (2.812 GHz)
   → Phase comparison at 2.812 GHz, signal chopped at ~12 kHz and synchronously detected

3. Fine Timing (~50 picosecond resolution; absolute, destructive)
   Aerogel cell generates Cerenkov radiation from single e- pulse
   Laser passes through optically transmissive Cerenkov cell
   → C1587 Streak Camera (Γ_t=2 psec) observes both signals

Laser and Electron Beam Timing and Position Overlap Diagnostics

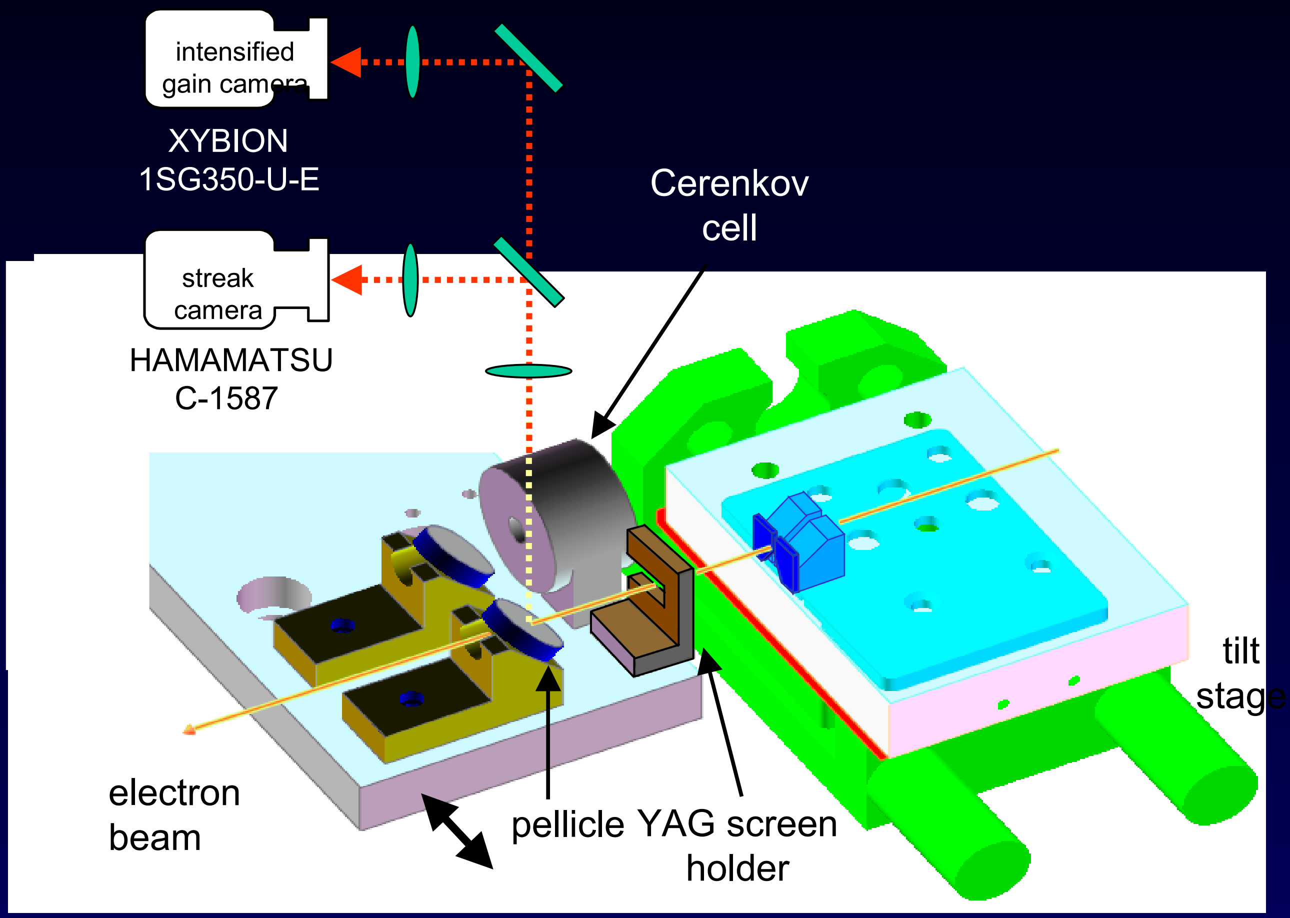

E163: Laser Acceleration of Electrons at the NLCTA

- Create an extraction line in a separate hall attached to the NLCTA to test candidate laser acceleration structures
  - Phase I: Install the LEAP Crossed-Gaussian accelerator, commission the beamline, and complete the physics study of interferometric (ITR) acceleration
  - Phase II: Install an IFEL prebuncher, and conduct the first acceleration experiments, using the LEAP cell, or candidate single-cell PBG structures

    → With the completion of Phase II, the facility will then host the world's highest brightness 0.8 μm electron injector
  - Phase III: Test multicell PBG structures

Experimental Requirements

Parameter	Value	Comment	Present Values at HEPL
Electron Beam Properties			
Bunch Charge	50 pC		**5 pC**
Beam Energy	60 MeV		**28 MeV**
Transverse Emittance	< 2.5 π mm-mr	Normalized	**10 π mm-mr**
Bunch Length	< 5 ps	FWHM	**~5 ps**
Energy Spread	< 20 keV	FWHM	**~20 keV**
Pulse Repetition Rate	10 Hz		**10 Hz**
Laser Beam Properties (for experiment)			
Pulse Energy	1 mJ		**1 mJ**
Pulse Wavelength	800 nm		**800 nm**
Pulse Length	0.1-10 ps	FWHM, variable	**1.0-10 ps**
Pulse Repetition Rate	10 Hz		**10 Hz**
Timing jitter w.r.t. electron beam	< 1 ps		**<3 ps**

E163 Layout

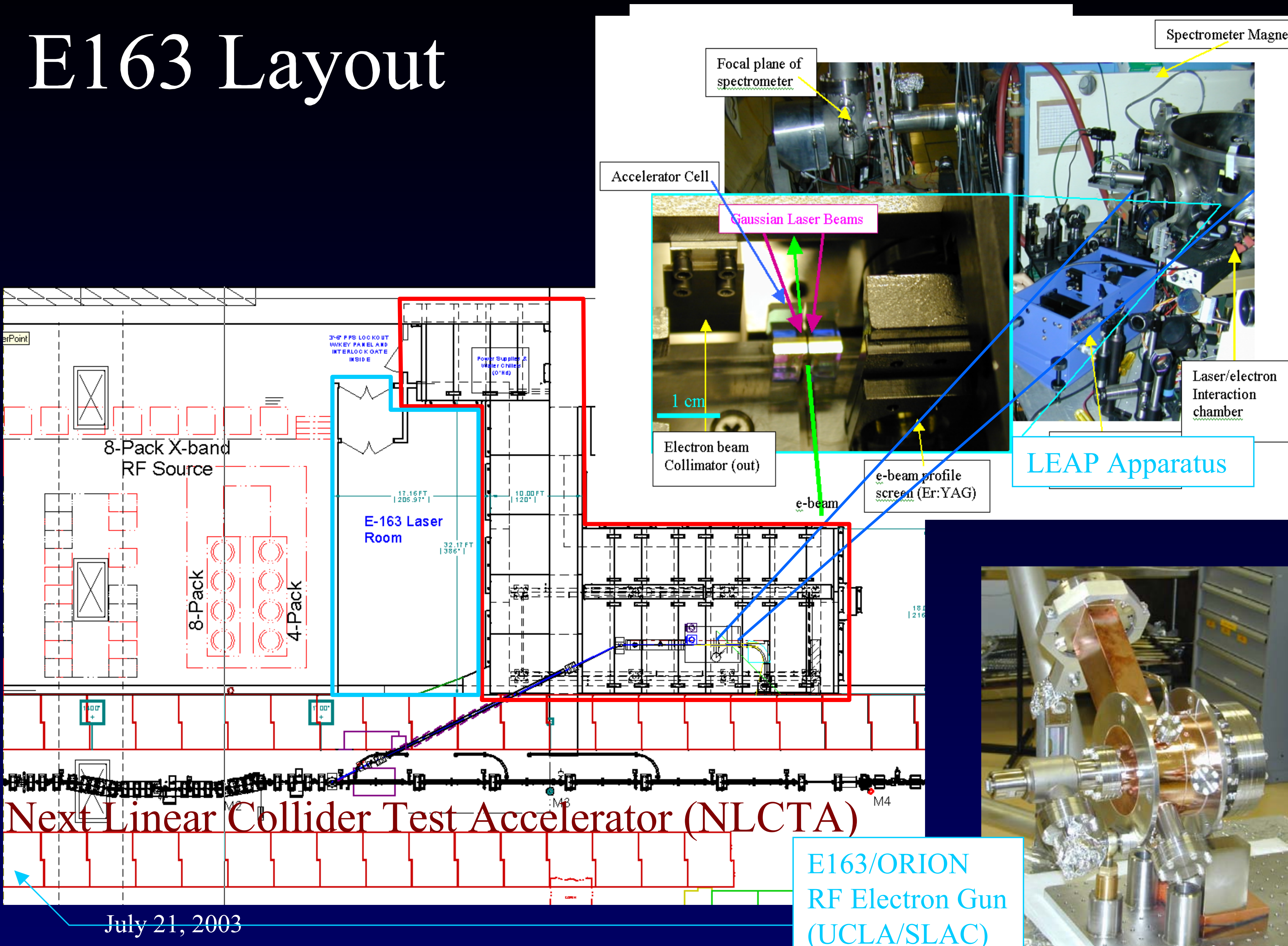

July 21, 2003

E163 End-to-end Simulation

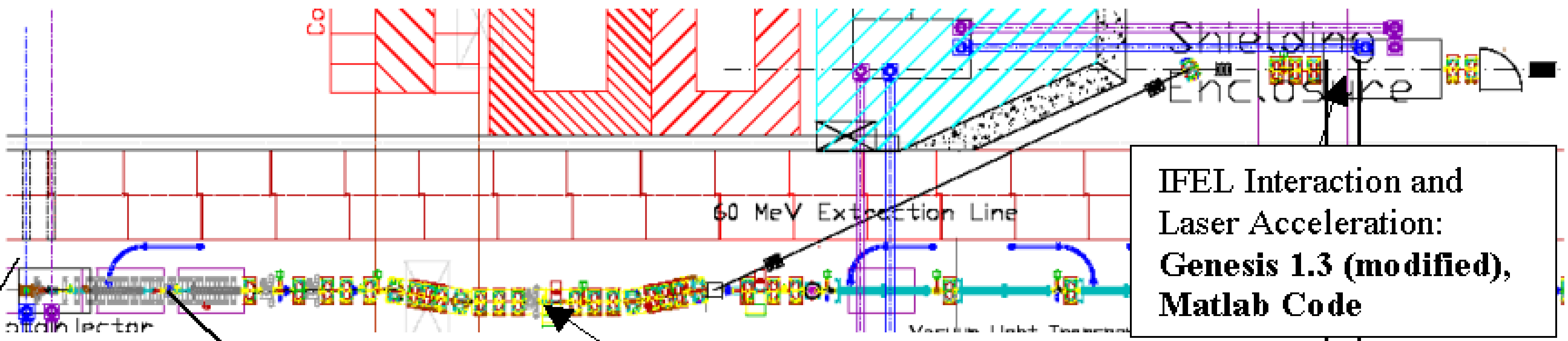

IFEL Interaction and Laser Acceleration: **Genesis 1.3 (modified), Matlab Code**

Electron generation and acceleration to 32.5 MeV: **Parmela** (UCLA/SLAC)

Electron transport through 2nd accelerator, chicane, dogleg, energy scraper: **Elegant 14.6β2**, with accelerator structure and collimator wakefields from analytic treatment in the NLC-ZDR, and initial magnet settings from 2nd-Order **Transport** optimization.

Remainder of Transport: **Elegant 14.6β2**

The LEAP Experimental Setup

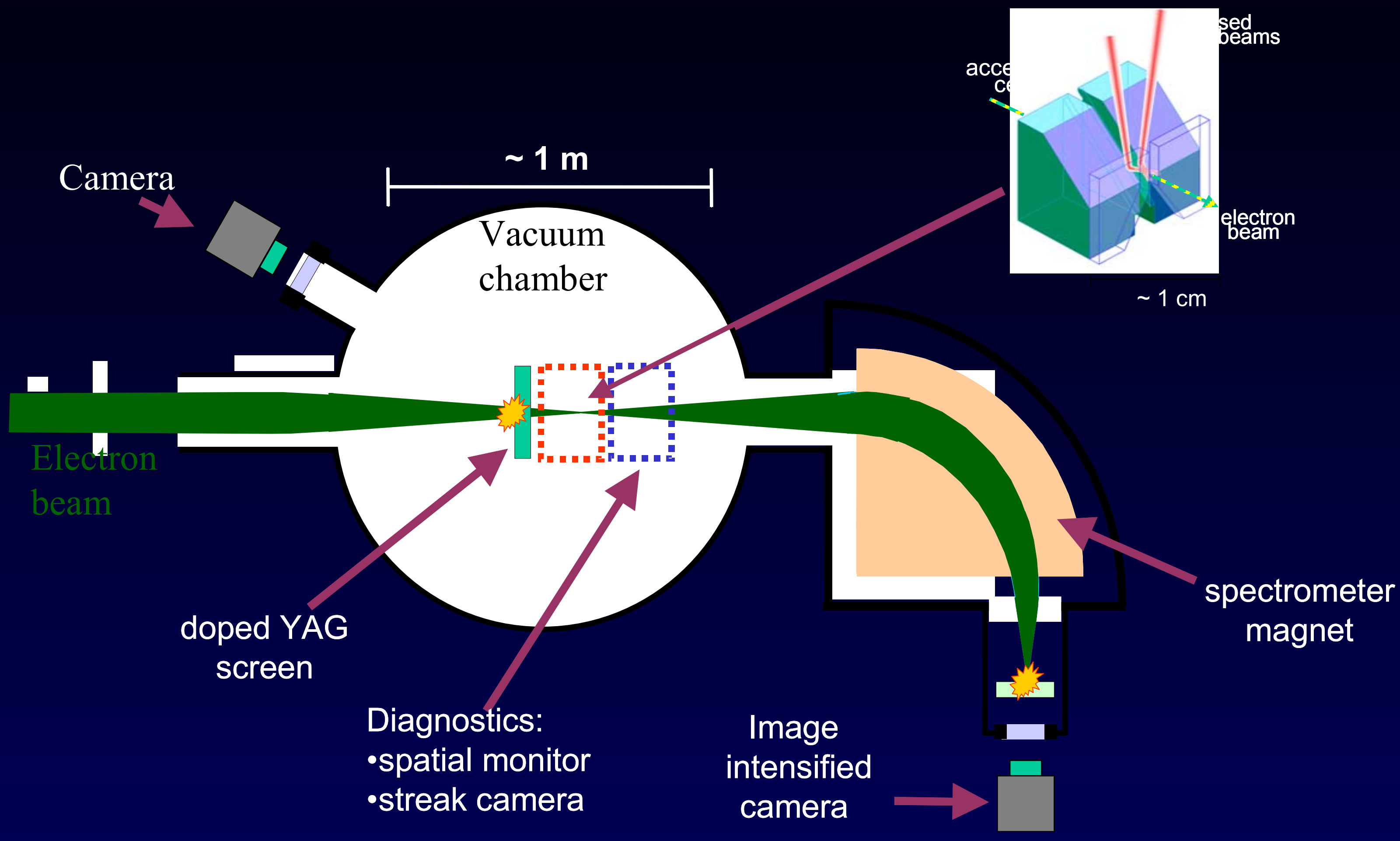

Anticipated Experimental Conditions

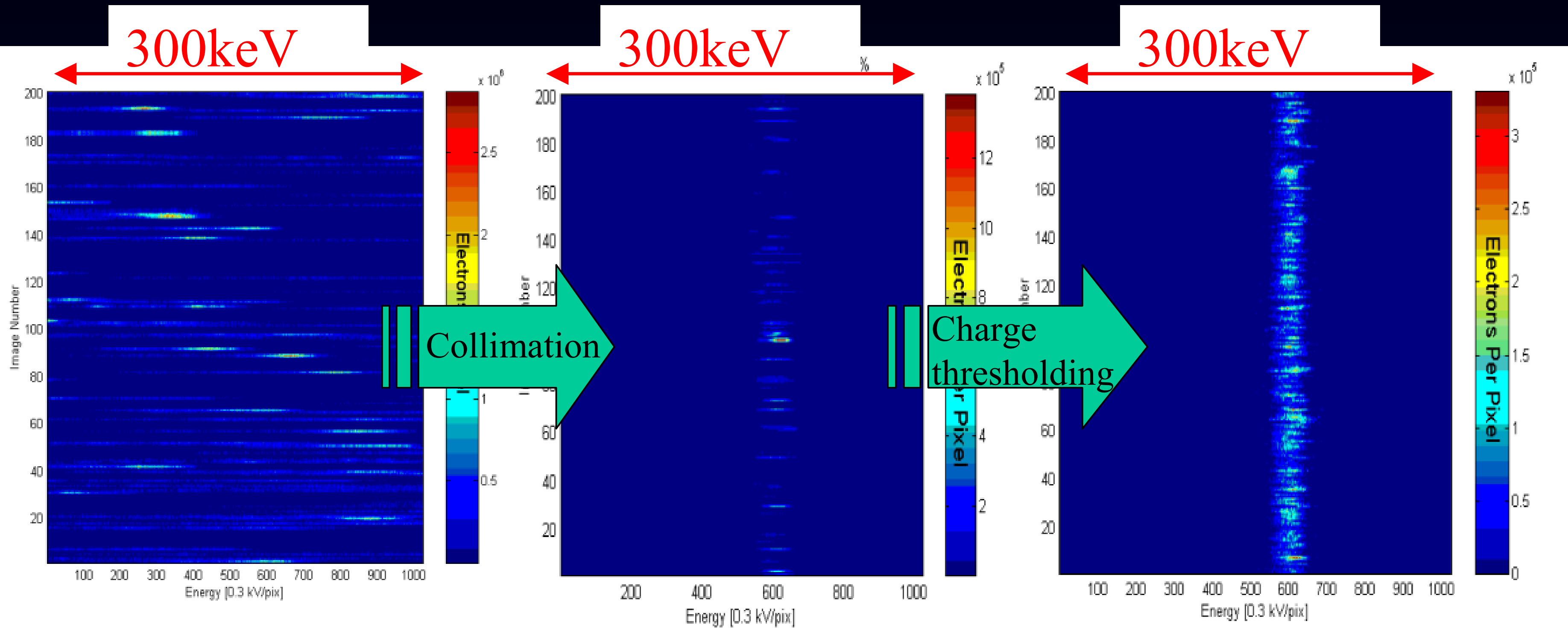

FIGURE 14. Null interaction time scan data sets: (left) with no collimation or charge thresholding, (center) with collimation only, and (right) with collimation and thresholding. Note that intensity per pixel has decreased an order of magnitude, but probe electron bunch has well defined energy characteristics. Bunch parameters and jitter are as in figures 12 and 13 above, but no laser interaction is present.

JITTERS ASSUMED: 5% Charge, 1% RF amplitude, 1 psec RF phase. (RMS).

Energy Collimator Installed at LEAP

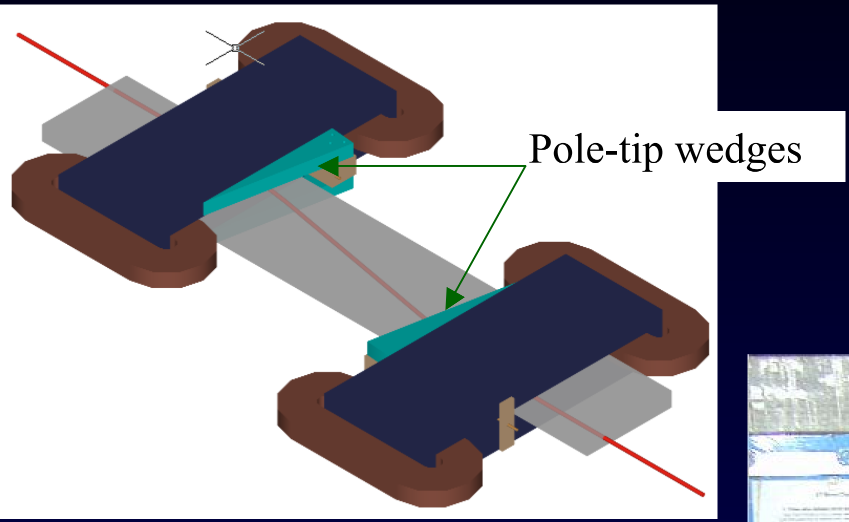

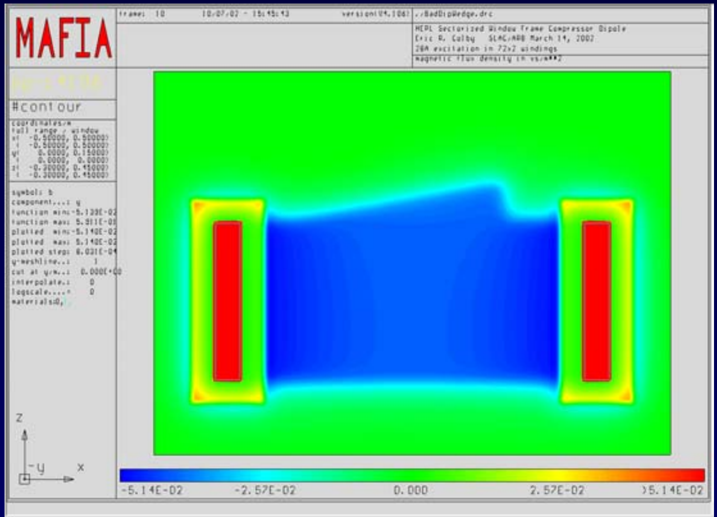

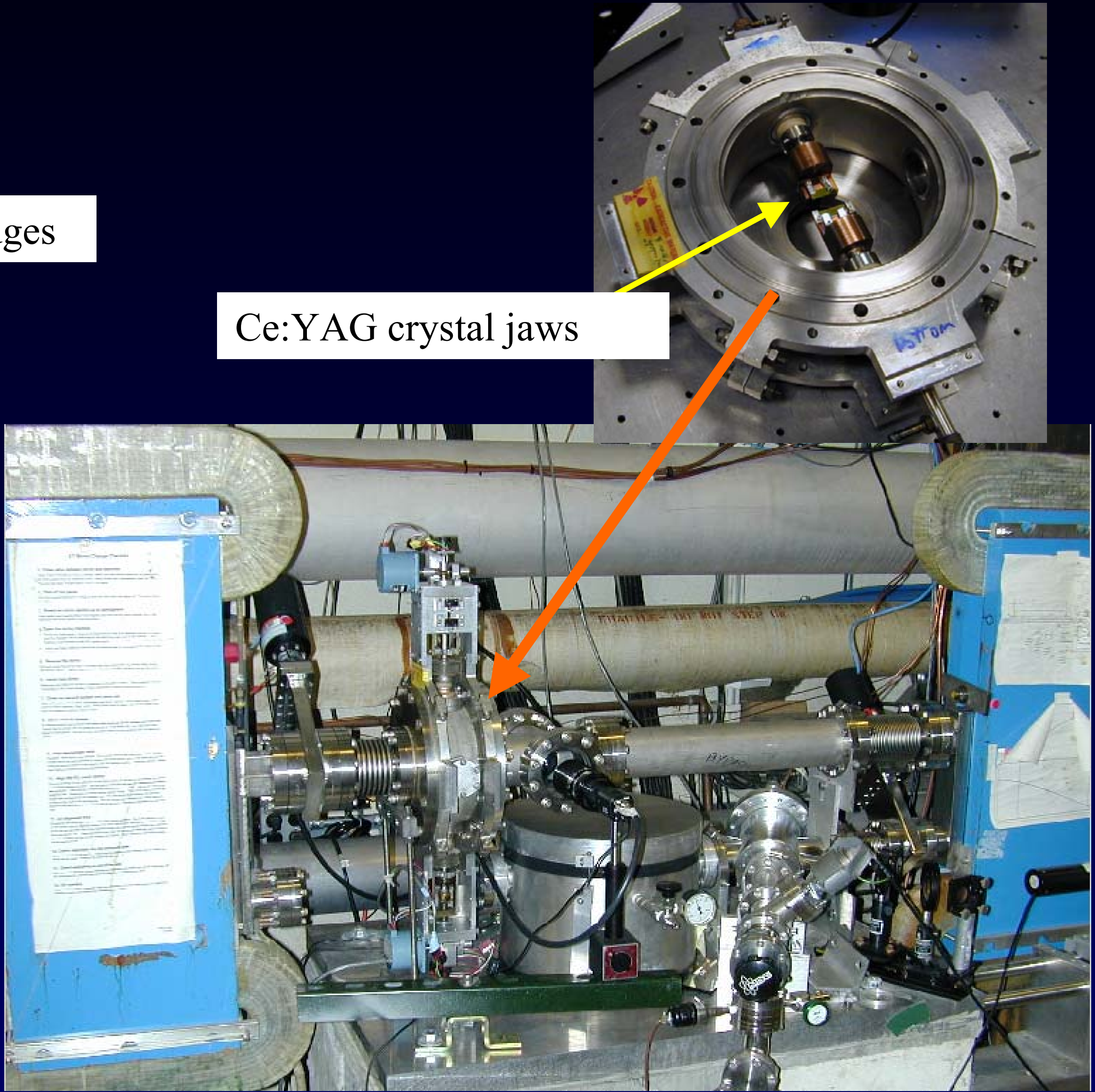

Results from Last LEAP Run (June 2002)

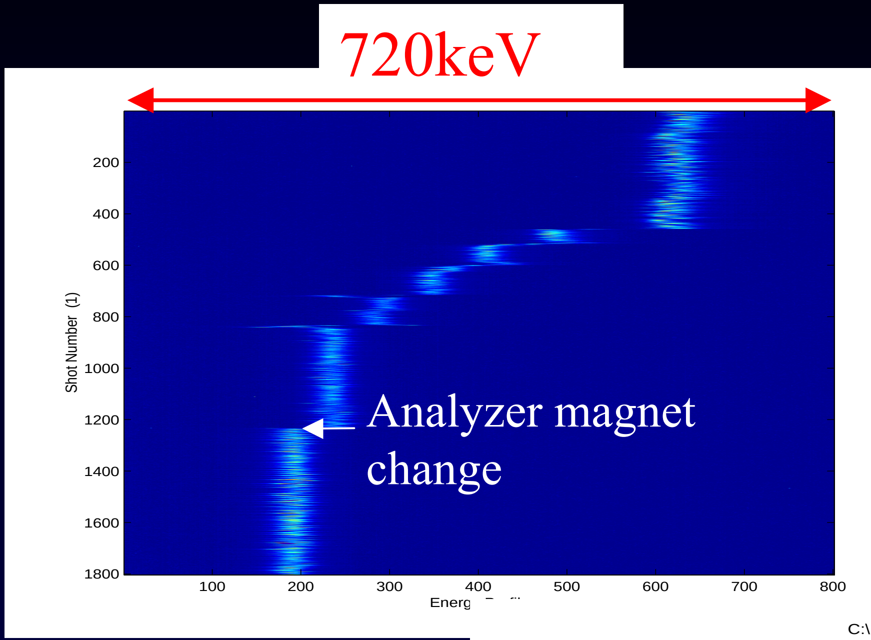

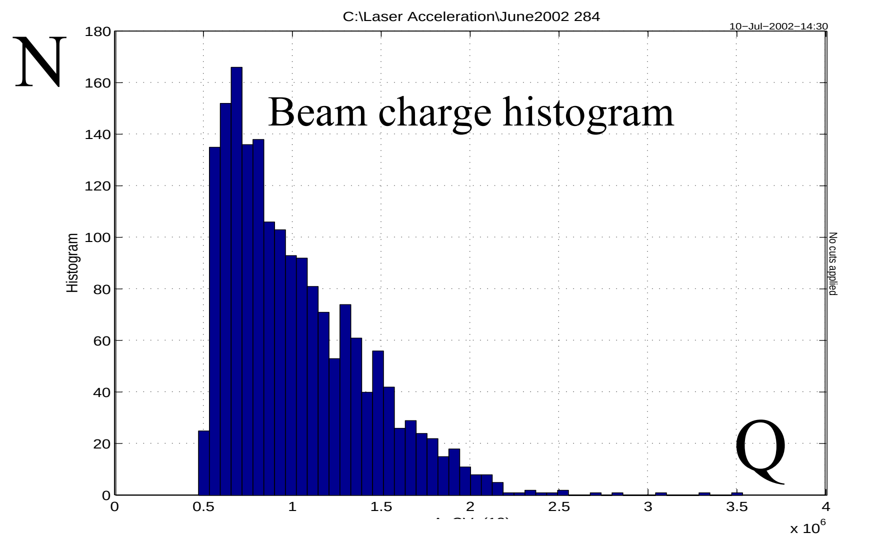

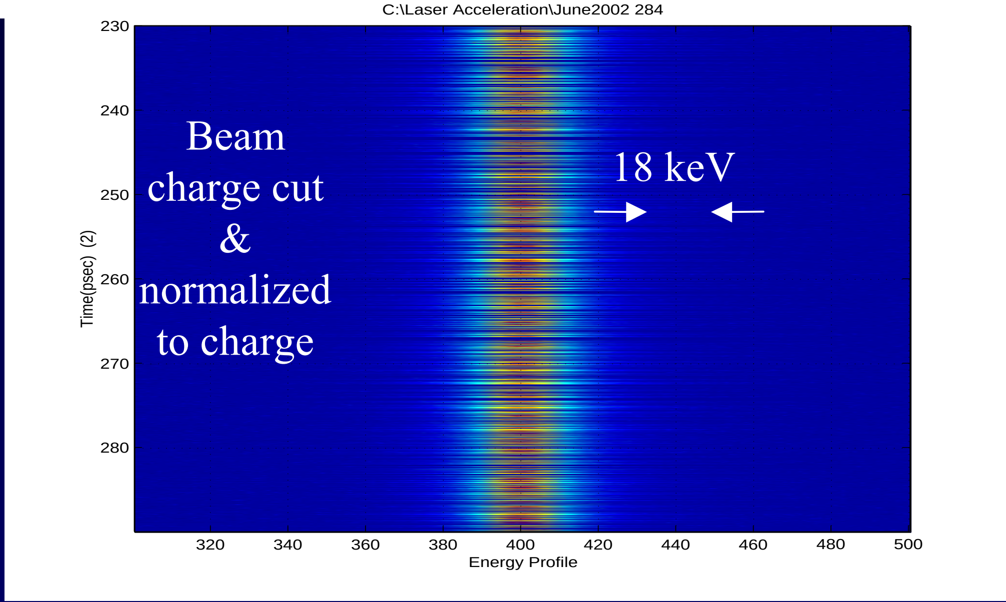

Simulated Optical Modulation Experiment (Phase I)

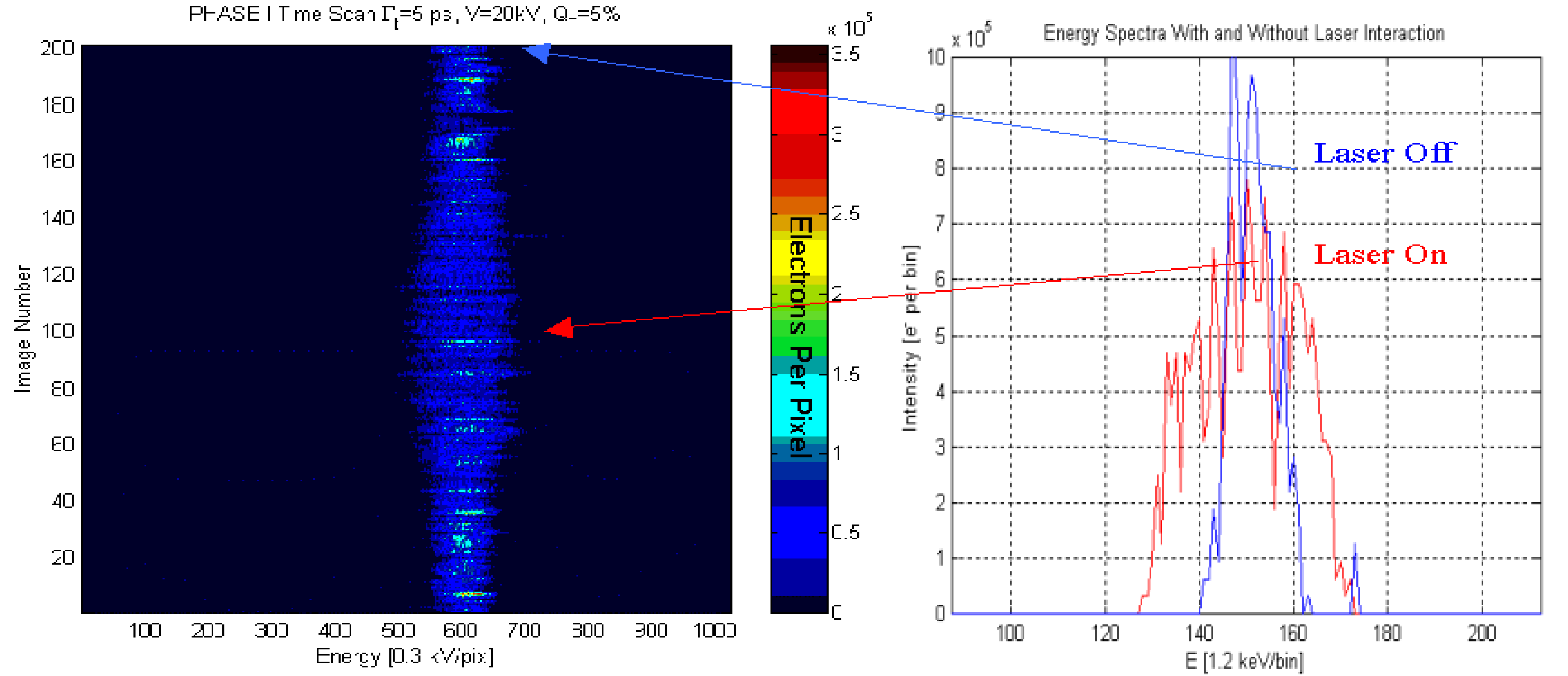

FIGURE 12. Simulated time scan data set (left), and comparison energy profiles for laser at full overlap (red) and out of time (blue), on an expanded scale. The relative timing between laser and electron bunch is swept from –5 psec to +5psec, with optimum overlap occurring at 0 psec (image #101). The laser pulse length is 5.0 ps FWHM, the laser-induced energy modulation amplitude is ±20 kV.

JITTER ASSUMED: 5% Charge, 1% RF amplitude, 1 psec RF phase. (RMS).

Simulated Optical Bunching and Acceleration Experiment (Phase II)

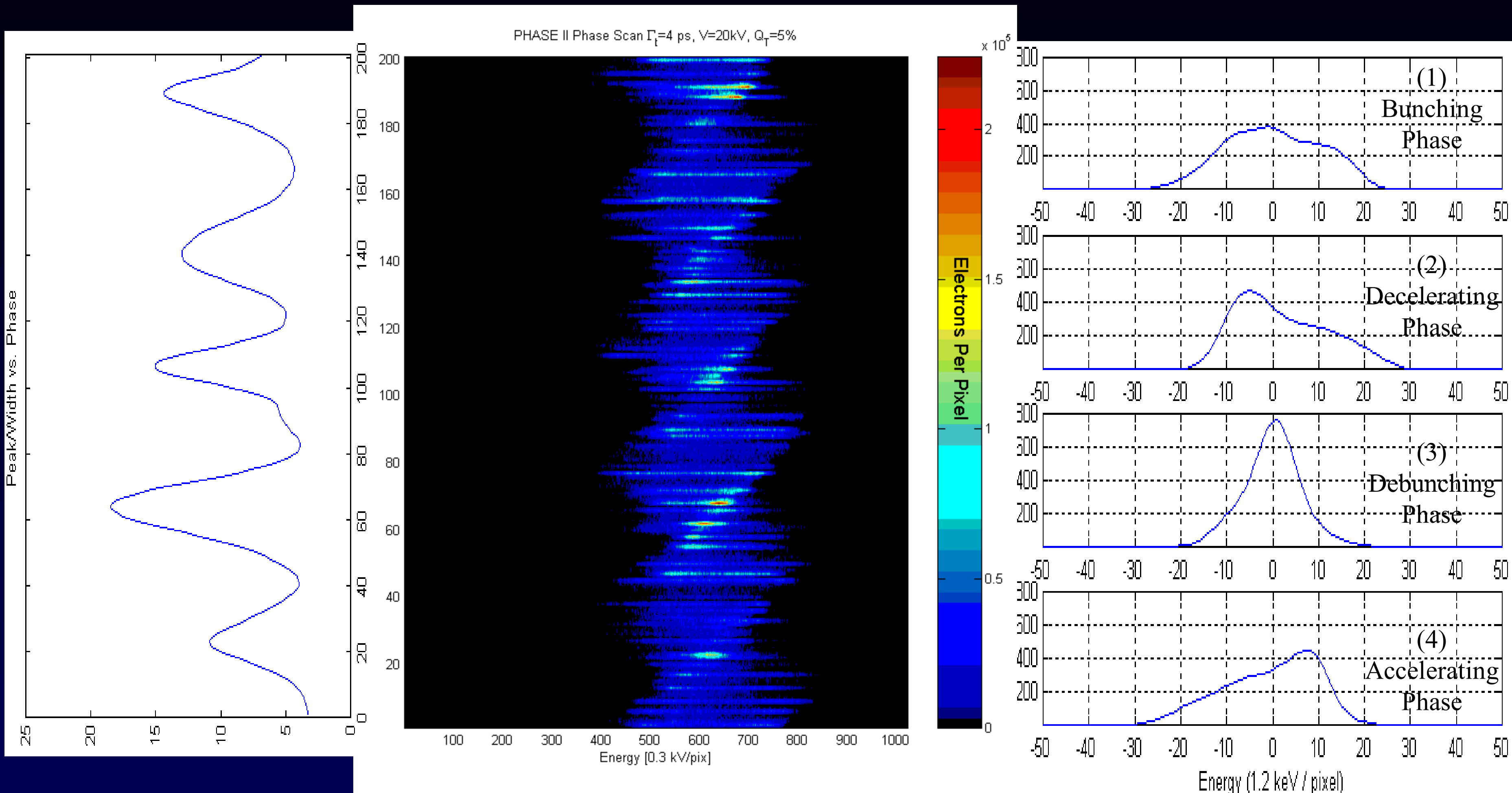

FIGURE 16. Charge density (left), simulated phase scan with jitter added (center), covering 10 π of variation in the relative phase between IFEL and laser accelerator, and averaged spectra (right) at (1) bunching, (2) decelerating, (3) debunching, and (4) accelerating phase.

JITTER ASSUMED: 1% RF amplitude, 1 psec RF phase, 5% Charge. (RMS).

E163 Lattice Error Sensitivity

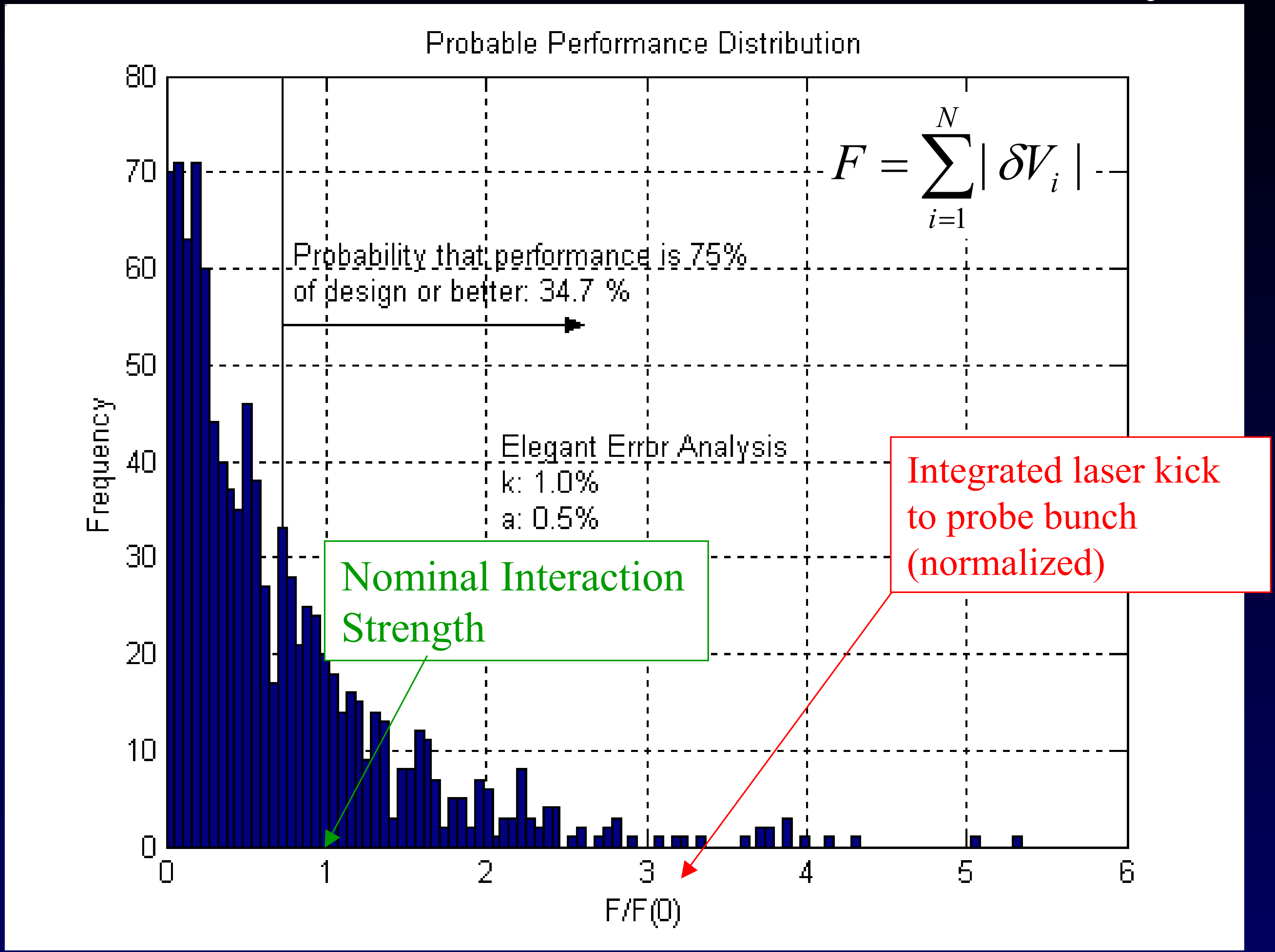

E163 Enclosure

7/16/03

↑Entrance labyrinth Inside↗

Outside→

Technical Roadmap

LEAP

1. Demonstrate the physics of laser acceleration in dielectric structures
2. Develop experimental techniques for handling and diagnosing picoCoulomb beams on picosecond timescales
3. Develop simple lithographic structures and test with beam

E163

Phase I. **Characterize laser/electron energy exchange in vacuum**

Phase II. **Demonstrate optical bunching and acceleration**

Phase III. **Test multicell lithographically produced structures**

Now and Future

1. Demonstrate carrier-phase lock of ultrafast lasers [NIST, Stanford]
2. Continue development of highly efficient DPSS-pumped broadband mode- and carrier-locked lasers [DARPA Proposal, SBIR Solicitation]
3. Devise power-efficient lithographic structures [SBIR Solicitation]
4. Devise stabilization and timing systems for large-scale machine [LIGO]
5. Much more!

Damage Threshold Improvement →

High Average Power Diode Pumped Solid State Lasers

Stanford University (SPRC)

Power Scaling with high spectral and spatial coherence

Research Objectives:

•to improve the efficiency of diode pumped solid state lasers such as in-band pumping, reduction of loss in the laser materials, improved pumped efficiency, and operation of phased array spatial mode lasers.

•to scale the average power while maintaining coherence by extending the master oscillator, power amplifier approach to encompass cw, energy storage, and ultrafast pulse format operation.

Stanford Research Program (DARPA)

A. High Average Power CW Lasers

B. High energy Yb:YAG lasers for Remote Sensing

C. High average power ultrafast lasers

D. Optical damage and plasma studies with ultrafast lasers

Conclusion

Rapid, market-driven development has pushed lasers into competitive standing with microwave tubes with regard to average power, efficiency, and control, but with peak powers and field strengths that are vastly superior.

Efficient power coupling between optical fields and beam must be demonstrated in an energy- and economically-scalable structure

→LEAP, E163, and the follow-on ORION VLA program

Continued laser development to produce lasers with **all** properties matched to accelerator requirements is needed

→DARPA-funded program at Stanford

Continued work on higher damage threshold, linear materials is highly desirable

→SPRC work on damage studies and optical ceramics

"One of the authors (W.W.H.), in his study of cavity resonators, was motivated by a desire to find a cheap method of obtaining high energy electrons. This cavity acceleration work was put aside, largely because of the change in standard of success caused by the advent of Kerst's betatron. . .

. . .By the end of the war many people were interested [in linear acceleration], possible reasons being: (a) wide-spread knowledge of cavity properties and technique, (b) the enormous pulsed powers made available by radar developments."

- E. L. Ginzton, W. W. Hansen, W. R. Kennedy, "A Linear Electron Accelerator", *Rev. Sci. Inst.,* **19**(2), p. 89, February 1948.

Final Thought